Calibration of the Fully Dynamic Rate Theory Using the Computer Code TRANSWELL

N. Ghoniem and G.L. Kulcinski

March 1977

UWFDM-200

FUSION TECHNOLOGY INSTITUTE

UNIVERSITY OF WISCONSIN

MADISON WISCONSIN

Calibration of the Fully Dynamic Rate Theory Using the Computer Code TRANSWELL

N. Ghoniem and G.L. Kulcinski

Fusion Technology Institute
University of Wisconsin
1500 Engineering Drive
Madison, WI 53706

http://fti.neep.wisc.edu

March 1977

UWFDM-200

"LEGAL NOTICE"

"This work was prepared by the University of Wisconsin as an account of work sponsored by the Electric Power Research Institute, Inc. ("EPRI"). Neither EPRI, members of EPRI, the University of Wisconsin, nor any person acting on behalf of either:

"a. Makes any warranty or representation, express or implied, with respect to the accuracy, completeness, or usefulness of the information contained in this report, or that the use of any information, apparatus, method, or process disclosed in this report may not infringe privately owned rights; or

"b. Assumes any liabilities with respect to the use of, or for damages resulting from the use of, any information, apparatus, method or process disclosed in this report."

Calibration of the Fully Dynamic Rate Theory Using the Computer Code TRANSWELL

N. Ghoniem
G. Kulcinski

March 1977

UWFDM-200

Fusion Technology Program
Nuclear Engineering Department
University of Wisconsin
Madison, Wisconsin 53706

Table of Contents

Abstract

A Fully Dynamic Rate Theory (FDRT), based on the Brailsford and Bullough Rate Theory, was developed previously to assess void growth in metals under transient and pulsed irradiation. The objective of the present paper is to examine the accuracy of this theory in two main aspects:

(a) Growth of voids during irradiation by comparing FDRT predictions to steady state irradiation data.

(b) Thermal shrinkage of voids (with no irradiation) by comparing FDRT predictions to void annealing experiments.

The theory is successful in explaining and predicting the high temperature metal swelling over a wide range of displacement rates ($\sim 10^{-6}$ to $\sim 10^{-1}$ dpa/sec) and with different bombarding species (neutrons, heavy ions and electrons) in three different metals (ST 316 Stainless Steel, Al and Ni). The FDRT approach is also shown to accurately describe void annealing in Al at different temperatures.

I. Introduction

The production of voids in metals during high temperature neutron, heavy ion and electron irradiation has been a subject of extensive experimental and theoretical investigation over the past 10 years. One of the more successful theories developed to describe the growth of voids is that based on Rate Theory and developed by Brailsford and Bullough (BB).[1] This theory is, however, limited to quasi-steady state conditions and is difficult to apply in a case where the microstructure and defect concentration is changing rapidly (e.g. in the first walls of inertially confined fusion reactors). The BB theory has been recently upgraded to deal with this limitation and has been converted into a Fully Dynamic Rate Theory (FDRT).[2] The computer code, TRANSWELL, based on this FDRT has also been described in a recent publication.[3] The purpose of the present paper is to show that TRANSWELL can simulate experimental data collected from several metals under greatly differing irradiation conditions. This "calibration" of the FDRT with steady state irradiated material is felt to be necessary before the FDRT can be extrapolated to pulsed irradiation conditions.

This report is organized in the following fashion. First, the philosophical approach for the calibration calculations is outlined and then the experimental data used for the comparisons is described. After a brief description of the FDRT and TRANSWELL Code, the theoretical predictions are compared to the experimental data. Finally, the additional information that comes from the TRANSWELL code is discussed and suggestions are made as to experimental data that might be reported and further improvements of the rate theory that could be made in the future.

II. Philosophy

Before examining the experimental data to be simulated and the actual simulation itself, it is worthwhile to state the philosophical approach taken here. It is certainly recognized that any successful theoretical model depends on a rather specific set of boundary conditions. In the case of the BB rate theory model, two of the most significant boundary conditions are: (1) that nucleation of new voids and interstitial loops has ceased and the existing microstructure is merely in a state of growth (one important exception to this statement is the fact that vacancy loops are continually being formed and dissolving[4]); (2) all of the sinks are homogeneously distributed in the metal. The latter assumption is easy to justify when the defect density and dpa rates are high.[1]

With these two conditions in mind, we proceeded to select some data from the open literature on three metals (316 SS, Al and Ni) irradiated with neutrons, heavy ions, and electrons. Even though there are a large number of studies on these materials (especially 316 SS) very few experimentalists measure and report all the data required to allow a reasonable comparison between theoretical models and the observed behavior. At a minimum, a successful growth model would require the following input - the saturation interstitial dislocation loop and void density, dpa rate, temperature, something about the displacement spike efficiency (e.g. single atom displacements by electrons vs large cascade spikes from neutron and heavy ions) and the appropriate material defect parameters. Two other assumptions were used in the simulation study: (1) The dose used in the simulation study corresponds to an actual dose measured after the incubation period for voids, (2) to separate nucleation from growth effects, we assume that after nucleation had ceased, the irradiation was turned off, and the solid returns to a thermal equilibrium. Then irradiation was turned on again to study the growth aspect of swelling. With this information,

two of the main outputs from the model are the growth rate of voids and dislocation loops. The resultant swelling is easily calculated from the void density. Unfortunately, even though the TRANSWELL code will predict the above parameters, as well as many more, there is very little experimental data in the literature which correlates both the dislocation loop and void parameters as a function of temperature, dpa rate and total damage level. We have attempted to find such data in the literature and use it for our calibration; however, where such data is unavailable, we had to supplement the experimental results with information from other studies or with an empirical fit to existing data.

It is also important to understand what happens during the transient stages when the irradiation is turned off, or on again. The buildup and decay of the vacancy and interstitial concentrations as well as the behavior of voids and loops between irradiation "pulses" can lend some understanding as to the ultimate response of the material. One of the crucial concepts in the application of FDRT to pulsed irradiation is that we allow voids to anneal out in between pulses when there is no damage produced. As part of the calibration procedure we have included a comparison between predicted and experimentally observed void annealing behavior.

Finally, when we have satisfied ourselves that the FDRT can be applied to the steady state irradiation case, as we have done in this report, we will extend the work into the pulsed irradiations regime in future publications.

III. Sources of Data

The TRANSWELL Computer Code is designed primarily for dealing with metals under pulsed or transient irradiations. The Fully Dynamic Rate Theory (FDRT), as it stands now, is a combination of ideas, some of which are directly supported experimentally while others are still not. A few pulsed experiments have been performed to date (5 , 6) under a restricted set of conditions, but because the problem is so complex, it is difficult to assess pulsed experiments without investigating the constituents of FDRT independently. Therefore, we must rely on steady state information.

In this section we will briefly present some experimental data on voids in metals which will be used to "calibrate" the FDRT and draw conclusions on the applicability of the theory as used in TRANSWELL. Experiments analyzed and presented here fall under two broad categories:

(1) Experiments to determine metal swelling under steady irradiation conditions.

(2) Experiments to determine void annealing behavior.

The first category of experiments will be invaluable in understanding microstructural changes during irradiation pulses, while the second will be important to assess void kinetics in between pulses.

III.A. Steady State Irradiation Experiments

(1) Solution Treated 316 SS

i.) Ion Irradiation

Williams[7] investigated the temperature dependence of void swelling in Type 316 austenitic stainless steel irradiated with carbon ions. Foils of Type 316 stainless steel containing 10 appm helium have been irradiated to a dose of 3×10^{17} ions/cm^2 at temperatures in the range 400°-700°C using 20 MeV C^{++} ions from the Harwell Variable Energy Cyclotron. This ion dose

produced an estimated maximum of 40 displacements/atom at 6.6 μm below the ion-incident surface. The void volume at each temperature was determined by transmission electron microscopy. In solution treated Type 316 steel, the void swelling reached a maximum of 12% at 600°C for a dose of 40 displacements/atom. The results of this work is shown in figure (1).

The void diameters and concentrations measured at a depth level of 6.6 μm and therefore corresponding to a damage concentration of 40 displacements per atom are listed in Table 1 as a function of irradiation temperature. These are average values, as there was some variation not only between equivalent specimens but also within a given specimen

Table 1 - Void sizes and densities in 20% cold worked and in 1050°C solution treated Type 316 steel resulting from a dose of 40 displacements per atom after prior implantation with 10^{-5} helium atoms per atom. (7)

Irradiation Temperature (°C)	Material Condition	Maximum Void Diameter (Å)	Minimum Void Diameter (Å)	Mean Void Diameter (Å)	Voids per cm^3
400	ST	~50	~30	~40	*
	CW	~50	~30	~40	*
450	ST	135	~30	85	1.1×10^{16}
	CW	~70	~30	~50	*
500	ST	300	65	210	3.0×10^{15}
	CW	310	80	180	4.2×10^{15}
550	ST	680	150	460	1.4×10^{15}
	CW	650	90	375	1.1×10^{15}
600	ST	800	200	490	1.4×10^{15}
	CW	680	100	385	1.0×10^{15}
650	ST	1100	170	710	4.2×10^{14}
	CW	1100	250	700	3.2×10^{14}
700	ST	1200	270	760	3.2×10^{14}
	CW	1200	300	800	2.8×10^{14}

* Insufficient voids resolved to make a realistic estimate

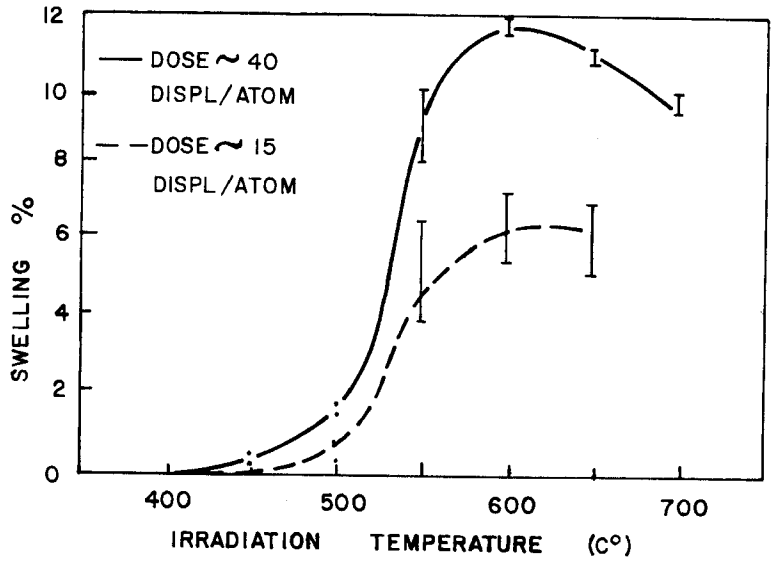

Fig. (1) Void swelling plotted as a function of temperature for solution treated Type 316 steel. (7)

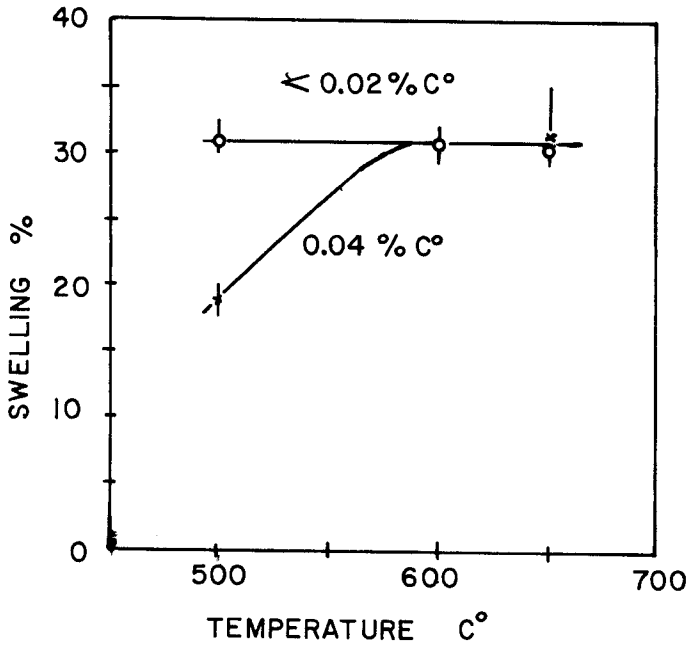

Fig. (2) The temperature dependence of the peak swelling during electron bombardment at 30 dpa.(8)

ii) Electron Irradiation

Makin and Walters[8] studied the effect of void density and carbon concentration on the swelling of type 316 austenitic steel irradiated in the HVEM. A representative selection of the results obtained as a function of temperature is shown in figures (2) and (3). It is shown that the presence of carbon has the effect of reducing swelling of stainless steel. The particular results we will refer to later are those for low carbon concentration, ~0.04%.

2. High Purity Aluminum

i) Neutron Irradiation

Packan[9] performed neutron irradiation experiments on pure aluminum in HFIR irradiation environment. Void formation in high purity aluminum resulting from irradiation to fluences between 1.5×10^{19} and 1.6×10^{22} neutrons/cm^2 (E>0.1 MeV) at a temperature of 55 ± 5°C was studied, primarily by means of transmission electron microscopy. Void size distribution curves were obtained for all fluences, and from these the mean void radius was found to increase in proportion to the irradiation time raised to the one-sixth power. The void concentration displayed a fluence dependence best described by a power law, $N_v \sim (\phi t)^{\alpha}$, in which the exponent decreased from 2.0 at 10^{19} neutrons/cm^2 down to only 0.1 at 10^{22} neutrons/cm^2. Treating the swelling with an analogous power relation, $\Delta V/V_o \sim (\phi t)^b$, a similar saturation effect was observed, with the fluence component b decreasing roughly from $\frac{5}{2}$ to $\frac{1}{2}$ over the range of fluence studied.

Experimental results of his work are shown in table (2) and figures (4), (5) and (6).

ii) Ion Irradiation

Irradiation of aluminum with 400 keV Al ions was carried out using the Harwell 500 KV Cockroft-Walton accelerator (Mazey (10)).

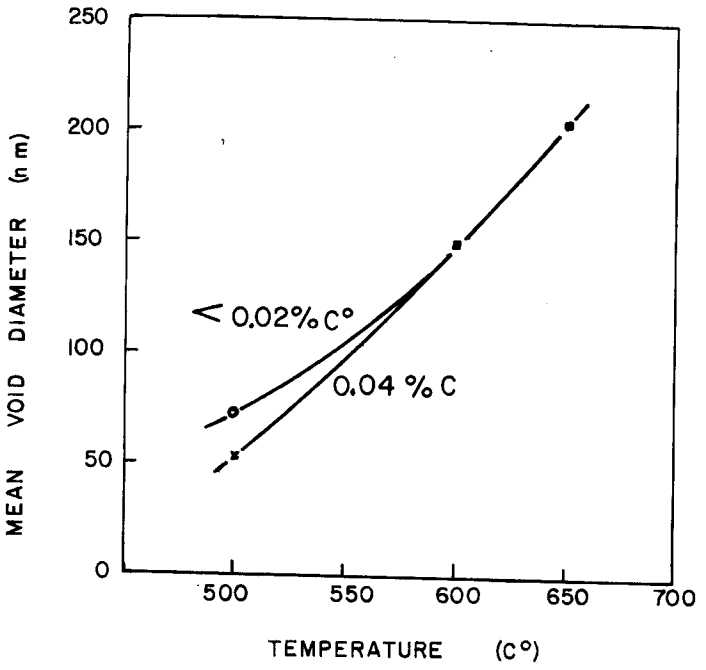

Fig. (3) The temperature dependence of the maximum mean void diameter after electron irradiation to 30 dpa.(8)

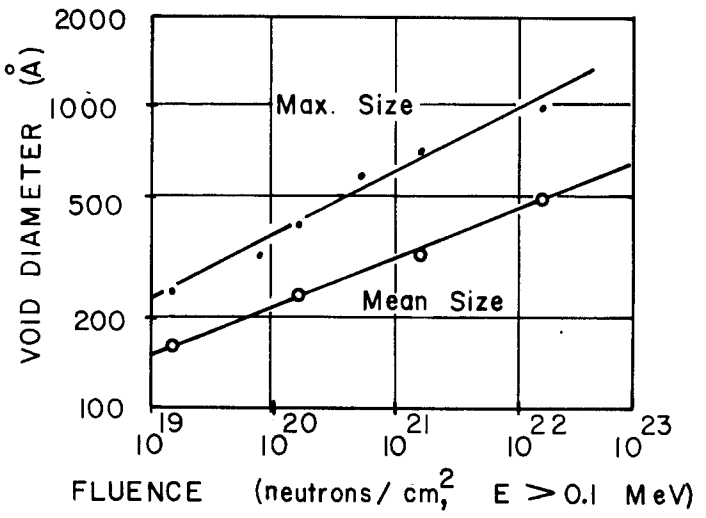

Fig. (4) Fluence dependence of the maximum and mean sizes of voids in neutron irradiated Al.(9)

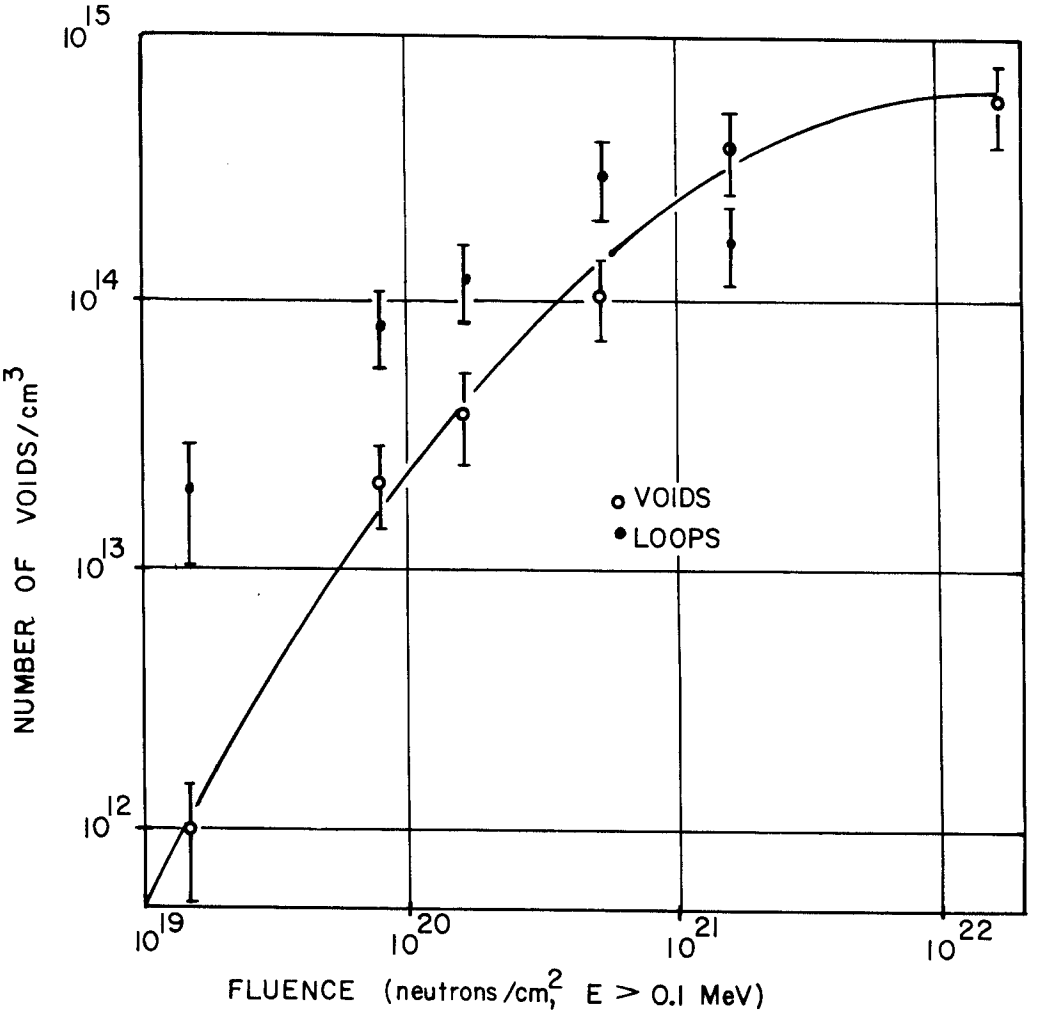

Fig. (5) Void concentration as a function of neutron fluence in Al.(9)

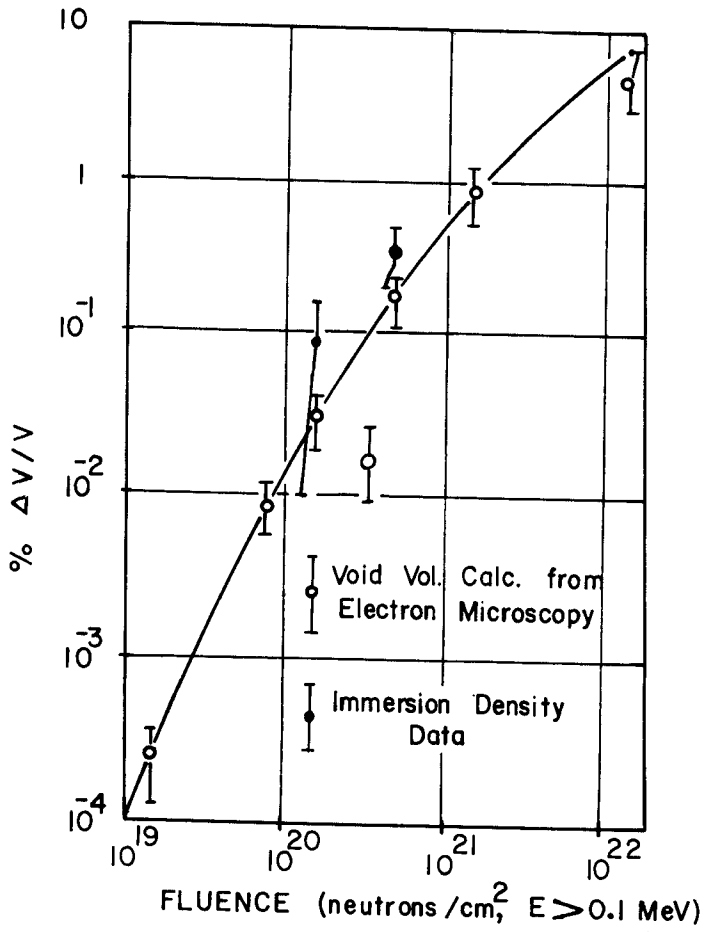

Fig. (6) Variation of the total void volume with fluence in Al.(9)

Table 2

Pertinent Data on Irradiation Effects in High Purity Aluminum[9]

Fluence (neutrons/cm^2 E > 0.1 MeV)	Void max. size (Å)	Void mean size (Å)	Number of voids/cm^3	Calc. total void volume (%)	Number of loops/cm^3
1.5×10^{19}	238	161	$\simeq 1 \times 10^{12}$	-	2×10^{13}
7.7×10^{19}	320	201	2.1×10^{13}	0.01	8 x 10 13
1.6×10^{20}	401	244	3.8×10^{13}	0.03	1×10^{11}
5.2×10^{20}	583	299	1.1×10^{14}	0.19	3×10^{14}
1.6×10^{21}	712	329	3.9×10^{14}	0.86	$\simeq 2 \times 10^{14}$
1.6×10^{22}	1020	495	5.9×10^{14}	7.4	-
1.3×10^{20} (Low flux)	609	323	1.9×10^{13}	0.04	5×10^{13}
5.3×10^{20} (degassed material)	532	279	1.0×10^{14}	0.15	-

The temperature-dependence of void swelling was investigated in non-helium doped 1100 grade aluminum by 400 keV Al^+ irradiation to 1×10^{17} ions/cm^2 at temperatures of 75, 100, 150, 200 and 250°C.

The dose-dependence of swelling was investigated at four dose levels in non-doped 1100 grade aluminum by irradiation with 400 keV Al^+ at 75°C. Details of void concentration and size and associated swelling are shown in Table (3) and plotted in Figure (7).

Table 3

Dose Dependence of Peak Swelling in Al at 75°C[10]

Specimen Number	Pre-Doping Treatment	Total Ion Dose x 10^{-17} cm^{-2}	Calculated Peak Dpa	Void Concentration x 10^{-15}cm^{-3}	$\bar{d}$ (Å)	Swelling %
C16	None	0.15	16	3.6	172	1.0
C3	None	0.625	65	4.6	219	2.6
C3	10^{-5} H	1.0	104	5.4	267	5.6
C17	None	1.5	156	12	227	8.4

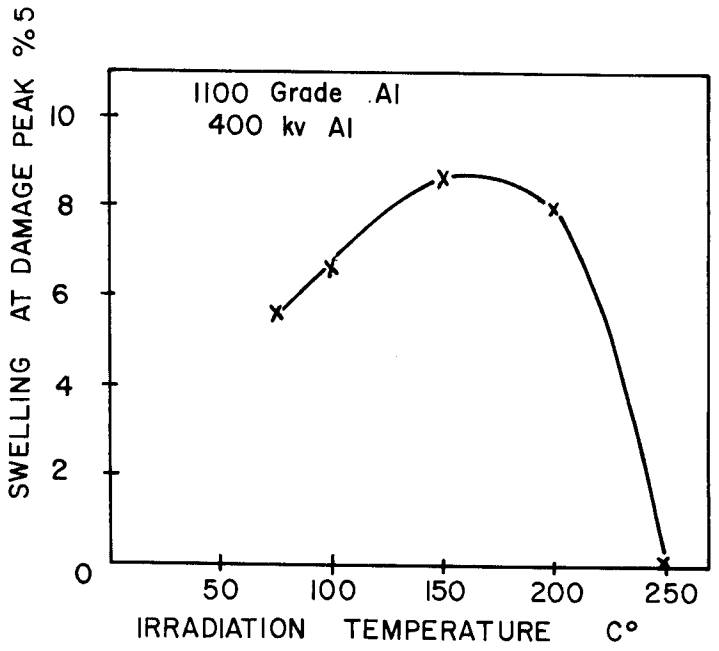

Fig. (7) Void swelling at damage peak as a function of temperature in 1100 grade Al Ion dose 1.0×10^{17} 400 keV Al^{+} cm^{-2} (104 dpa at peak).[10]

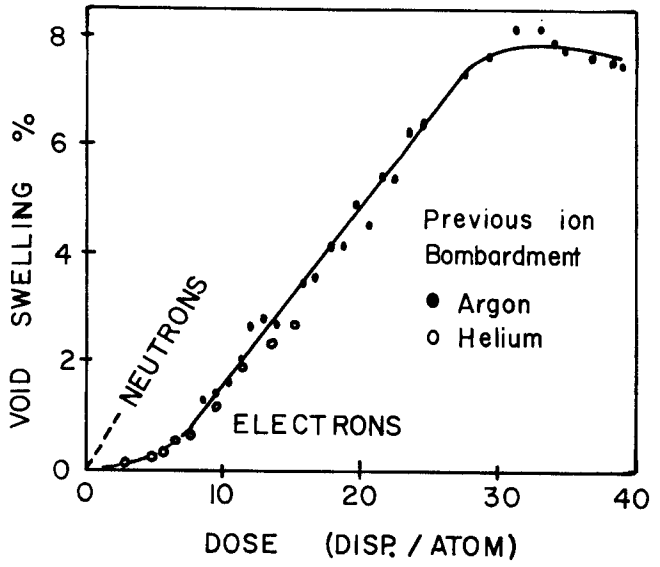

Fig. (8) Void swelling in nickel versus dose at 450°C including data from neutron irradiation at 430°C.[12]

3. High Purity Nickel

i) Ion Irradiated

The temperature dependence of void and dislocation loop structures was studied by Sprague et al. (11) in high-purity nickel irradiated with 2.8 MeV $^{58}Ni^{+}$ ions to a displacement density of 13 displacements per atom (dpa) at a displacement rate of 7×10^{-2} dpa/sec over the temperature range 325°C to 625°C. Dislocation loops with no significant concentrations of voids were observed in specimens irradiated at 475°C and below. Specimens irradiated between 525°C and 725°C contained both voids and dislocations. The maximum swelling was measured as 1.2% at 625°C. Results obtained from this experiment are summarized in table (4). No helium doping was used in this work.

Table 4

Effect Of Irradiation Temperature On Voids And Dislocations In Nickel (11)

Irrad. Temp. (°C)	Void Density (cm^{-3})	Mean Void Diameter (Å)	Std. Dev. Of Diameter (Å)	Swelling (%)	Dislocation Density (cm^{-2})
375	-	-	-	-	7.8×10^{10}
425	-	-	-	-	4.5×10^{10}
475	-	-	-	-	4.5×10^{10}
525	7.6×10^{15}	100	20	0.48	2.9×10^{10}
575	6.9×10^{15}	130	20	0.90	2.0×10^{10}
625	1.8×10^{15}	225	45	1.2	5.6×10^{9}
675	3.0×10^{13}	725	145	0.62	2.8×10^{9}
725	1.4×10^{13}	800	120	0.40	1.6×10^{9}

ii) Electron Irradiated

Voids in nickel electron irradiated at 450°C were studied by Norris.[12,13] The specimen was previously bombarded with 6×10^{17} He^+ ions/m^2 at 50 keV and then annealed at 640°C to remove the vacancy clusters. A calculated displacement rate of 2.06×10^{-3} dpa/sec with an error of ±20% was used. Figure (8) shows the results of this experiment with dose uncertainty of ±20% and swelling uncertainty of ±30%. Swelling saturation at high doses is suspected to be due to surface effects in thin foils.

III.B. Void Annealing Experiments

(i) Westmacott, Smallman and Dobson's Experiment[14]

Octahedral voids up to 500 Å in diameter were produced in thin foils of spectroscopically pure aluminum by quenching. Transmission electron microscopy has been used to investigate the thermal stability of these voids and it was observed that they anneal out rapidly in the range of 150-200°C. The annealing treatments were performed outside the microscope in a silicon-oil bath controlled to an accuracy of ± 0.25°C. At best, the error in their method was estimated to an accuracy of ±10 Å in diameter. The experimental curve produced is shown in figure (9). By adopting a value of the diffusion coefficient determined by Volin and Balluffi,[15] they were able to estimate a surface energy of $\gamma_s = 1140 \pm 200$ ergs/cm^2.

(ii) Volin and Balluffi's Experiment[15]

The annealing kinetics of voids in 99.9999 wt % pure aluminum were studied over the temperature range 85 to 209°C in thin specimens by transmission electron microscopy. The isothermal shrinkage of individual voids was measured and interpreted on the basis of a self-diffusion annealing model. The self-diffusion coefficient of aluminum, as determined from the data, was given by

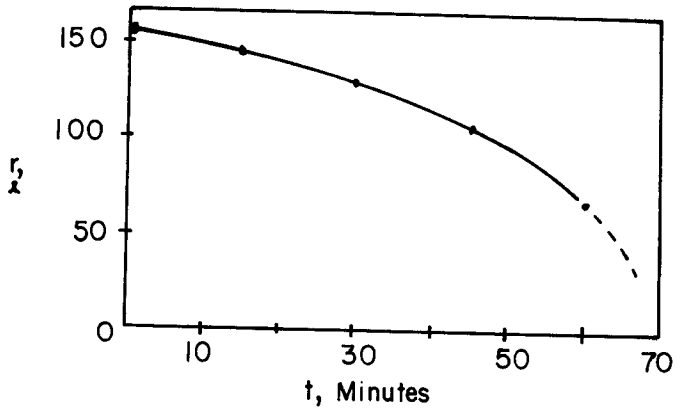

Fig. (9) Radius-time curve for void annealing in aluminum at 175°C (after Westmacott et al. (14))

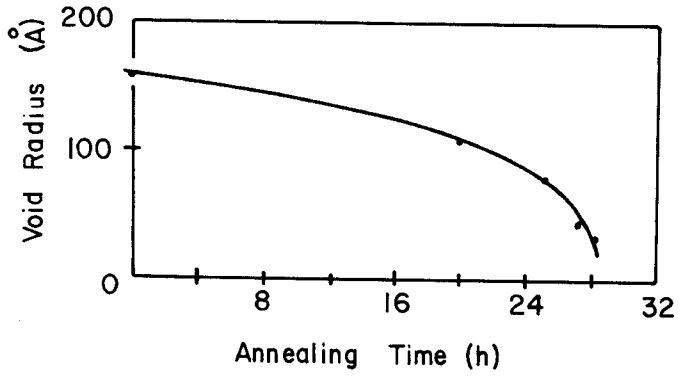

Fig. (10) Annealing of voids in aluminum at 126°C (after Volin and Balluffi (15))

D_s = 0.176 ergs (-1.31 eV/kT) $cm^2 s^{-1}$. The activation energy, Q = 1.31 eV, was found to be significantly lower than the value Q = 1.48 eV determined by Lundy and Murdock[19] at temperatures near the melting point in a radioactive tracer technique. In all their calculations, the surface energy of aluminum was assumed to be γ_s = 1500 ergs/cm^2, and the atomic volume was taken as $\Omega = 16.6 \times 10^{-24} cm^{-3}$. Figure (10) shows the annealing behavior of voids at 126°C.

IV. TRANSWELL Computer Code Results

IV. A.) Description of the Computer Code

The TRANSWELL Code solves the kinetic rate equations for single vacancies and single interstitials in a homogeneous medium (spatially averaged concentrations). Coupled rate equations are solved for an average void radius, average aligned and non aligned loop radii, the concentration of aligned and non aligned vacancy loops, the concentration of vacancies tied up in aligned and non aligned vacancy loops, and finally strain and strain rate equations. The code is built on the theoretical ideas in the chemical rate kinetics formulation developed by Harkness and Li (16); Wiedersich (17); Brailsford and Bullough (1); Bullough, Eyre and Krishan (4); and Ghoniem and Kulcinski (2). The code was basically designed for the very rapid response of metals under irradiation as in the pulsed irradiation example initially studied in reference (18). The sensitivity of such studies to different input parameters is a prime motive for the "calibration" of different aspects of the model.

A detailed analysis of the Computer Code is found in reference (3) while a description of the underlying theory is in reference (2).

IV. B. Results of TRANSWELL on Void Growth

The flexibility of the Computer Code TRANSWELL allows the study of a metals response to irradiation under a wide variety of conditions. In this paper, emphasis will be cast on correlating specific experimental observations with TRANSWELL simulations. Parametric studies of the effects of different material and irradiation variables will be postponed to a later publication. However, a limited amount of supporting information, that lead to understanding of swelling behavior, will be presented here.

In all the computer simulations studied we assumed the following:

a. A simple temperature dependent nucleation relationship for the number densities of voids and interstitial loops at saturation of the form:

$$N_v^s = N_v^o \exp \{E_v(eV)/kT\}$$

$$N_{i\ell}^s = N_{i\ell}^o \exp \{E_{i\ell}(eV)/kT\}$$

where N_v^o, $N_{i\ell}^o$, E_v and $E_{i\ell}$ are experimentally determined or computer fitted quantities.

b. Initial "free-growth" void radius defined as that radius at which a void can freely grow at a certain temperature without the assistance of internal gas pressure.

c. Initial vacancy loop radius determined by the number of vacancies in a collision cascade (about 15 Å).

d. A dislocation interstitial bias factor (Z_i) adjusted to fit the metal's swelling behavior under all conditions.

The following notations for metal parameters were used:

E_v^f = Vacancy formation energy in eV.

E_i^f = Interstitial formation energy in eV.

D_v^e = Vacancy diffusion coefficient preexponential in cm^2/sec.

D_i^e = Interstitial diffusion coefficient preexponential in cm^2/sec.

E_v^m = Vacancy migration energy in eV.

E_i^m = Interstitial migration energy in eV.

b = Burger's vector in cm.

γ = Surface energy in eV/cm^2.

Z_v = Vacancy-dislocation bias factor.

Z_i = Interstitial-dislocation bias factor.

Ω = Atomic volume in cm^3.

γ_{sf} = Stacking falut energy in eV/cm^2.

μ = Shear modulus in $ergs/cm^3$

ν = Poisson's ratio

e_v = Vacancy relaxation volume in cm^3.

e_i = Interstitial relaxation volume in cm^3.

α = Interstitial-vacancy recombination coefficient.

Table (5) gives values of these parameters for the three investigated metals.

Table 5

Metals Parameters for Steel, Aluminum and Nickel

Used For Comparison of Experimental Results to TRANSWELL

Parameter	Units	Steel	Aluminum	Nickel
E_v^f	eV	1.60	0.66	1.39
E_i^f	eV	4.00	3.20	4.08
E_v^m	eV	1.30	0.57	1.38
E_i^m	eV	.20	0.10	0.1
D_v^e	cm^2s^{-1}	.58	0.04	0.1
D_i^e	cm^2s^{-1}	10^{-3}	0.08	0.12
b	cm	2×10^{-8}	2.32×10^{-8}	2.5
γ	$ergs/cm^2$	1.25×10^{15}	6.2415×10^{14}	1.25×10^{15}
Z_v	-	1.00	1.00	1.00
Z_i	-	1.08	1.015	1.022
Ω	cm^3	0.8×10^{-23}	1.25×10^{-23}	1.5625×10^{-23}
γ_{sf}	$ergs/cm^2$	9.4×10^{12}	1.7476×10^{14}	2.496×10^{14}
μ	$dynes/cm^2$	2.836×10^{11}	2.65×10^{11}	9.47×10^{11}
ν	-	0.291	0.347	0.276
e_v	cm^3	-0.16×10^{-23}	-0.25×10^{-23}	-0.3125×10^{-23}
e_i	cm^3	1.12×10^{-23}	1.75×10^{-23}	2.1875×10^{-23}
$\frac{\alpha}{D_i}$	-	10^{16}	10^{16}	10^{15}
ε^*	-	0.044	0.001	0.01

* For ion or neutron irradiation only

(1) Solution Treated 316 SS

i) Ion Irradiation

Experimentally measured void concentrations as a function of temperature were fitted in the present work, to the expression:

$$N_v^s = 3.15 \times 10^{11} \exp\{0.625 \text{ eV}/kT\},$$

while the interstitial loop number densities were generated from the expression:

$$N_{i\ell}^s = 1.34 \times 10^{-4} \exp\{2.8 \text{ eV}/kT\}$$

The following initial conditions were assumed:

initial void radius = 40 Å

initial vacancy loop radius = 15 Å

number of gas atoms in a void = 100

cascade efficiency[10] = 0.044 }
bias factor[10] = 1.08 } *

The initial interstitial loop radius was calculated from the condition:

number of vacancies in visible defect clusters = number of interstitials in visible defect clusters

$$3.15 \times 10^{11} \exp[0.625/kT] \cdot \frac{4}{3} \pi r_{vo}^3 = 1.34 \times 10^{-4} \exp[2.8/kT] \cdot \pi r_{i\ell o}^2 b$$

where,

r_{vo} = initial void radius

$r_{i\ell o}$ = initial interstitial loop radius

The temperature dependent swelling of ST 316 SS is compared with experiment in figure (11). Notice that the computer results tend to be lower than experimentally measured swelling at high temperatures. This is due to the fact that voids, starting with a small initial void radius, tend to shrink faster at high temperatures. This behavior at high temperature will be

*The calibration is not dependent on the individual values of ε or Z_i but rather the combination of values. For example, $Z_i = 1.025$ and $\varepsilon = 1.2\%$ would give roughly the same results (see apendix A).

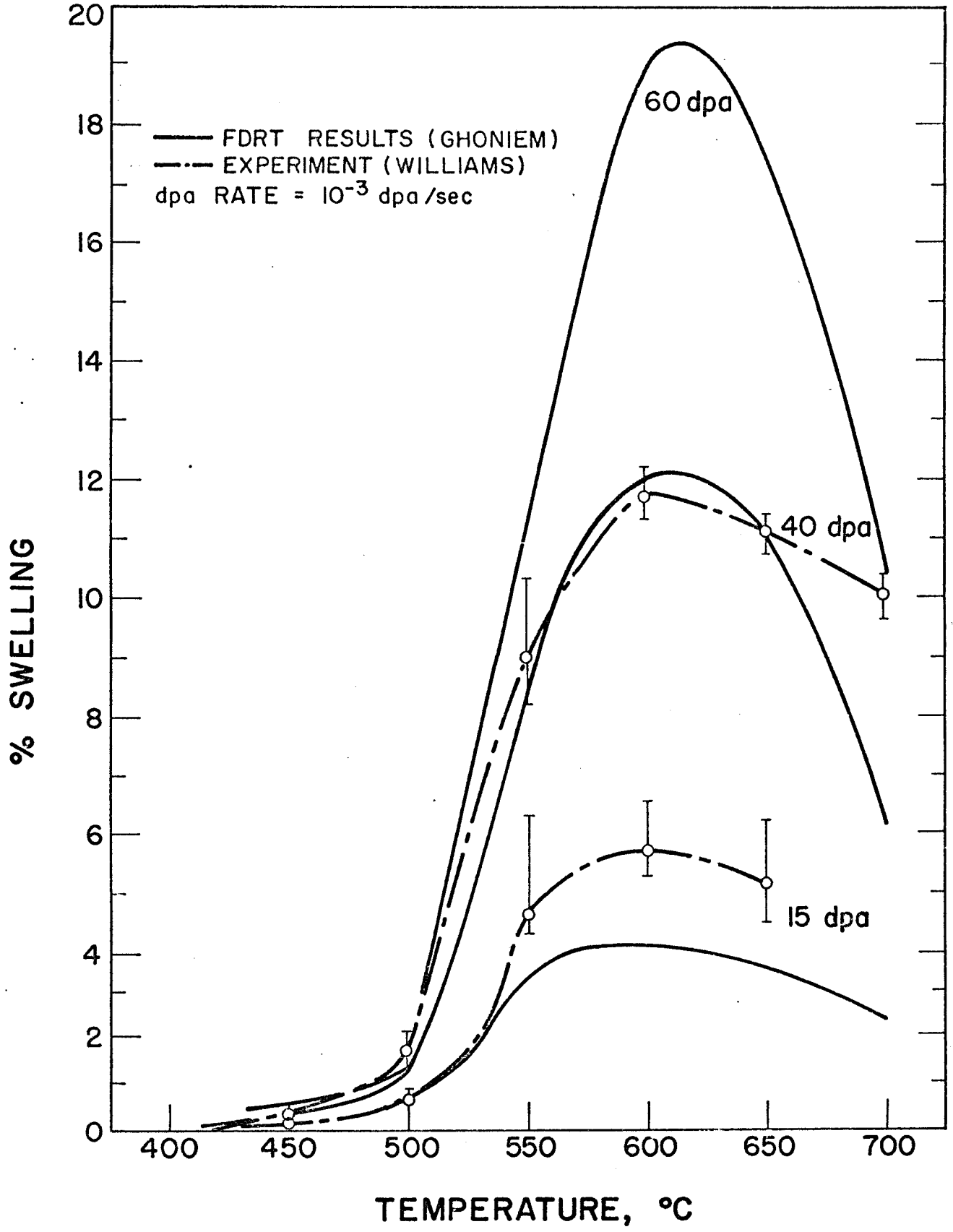

Fig.(11) COMPARISON BETWEEN THE FULLY DYNAMIC RATE THEORY (FDRT) AND EXPERIMENTAL RESULTS FROM T.M. WILLIAMS (AERE HARWELL). THE TEMPERATURE DEPENDENCE OF VOID SWELLING IN M316 S.S. IRRADIATED WITH 22 MeV C^{++} IONS.

Fig.(12) COMPARISON BETWEEN THE FULLY DYNAMIC RATE THEORY (FDRT) AND EXPERIMENTAL RESULTS FROM T.M. WILLIAMS (AERE HARWELL). THE TEMPERATURE DEPENDENCE OF VOID DIAMETER AS A FUNCTION OF TEMPERATURE AT 40 dpa IN SOLUTION TREATED M316 S.S. IRRADIATED WITH 22 MeV C^{++} IONS.

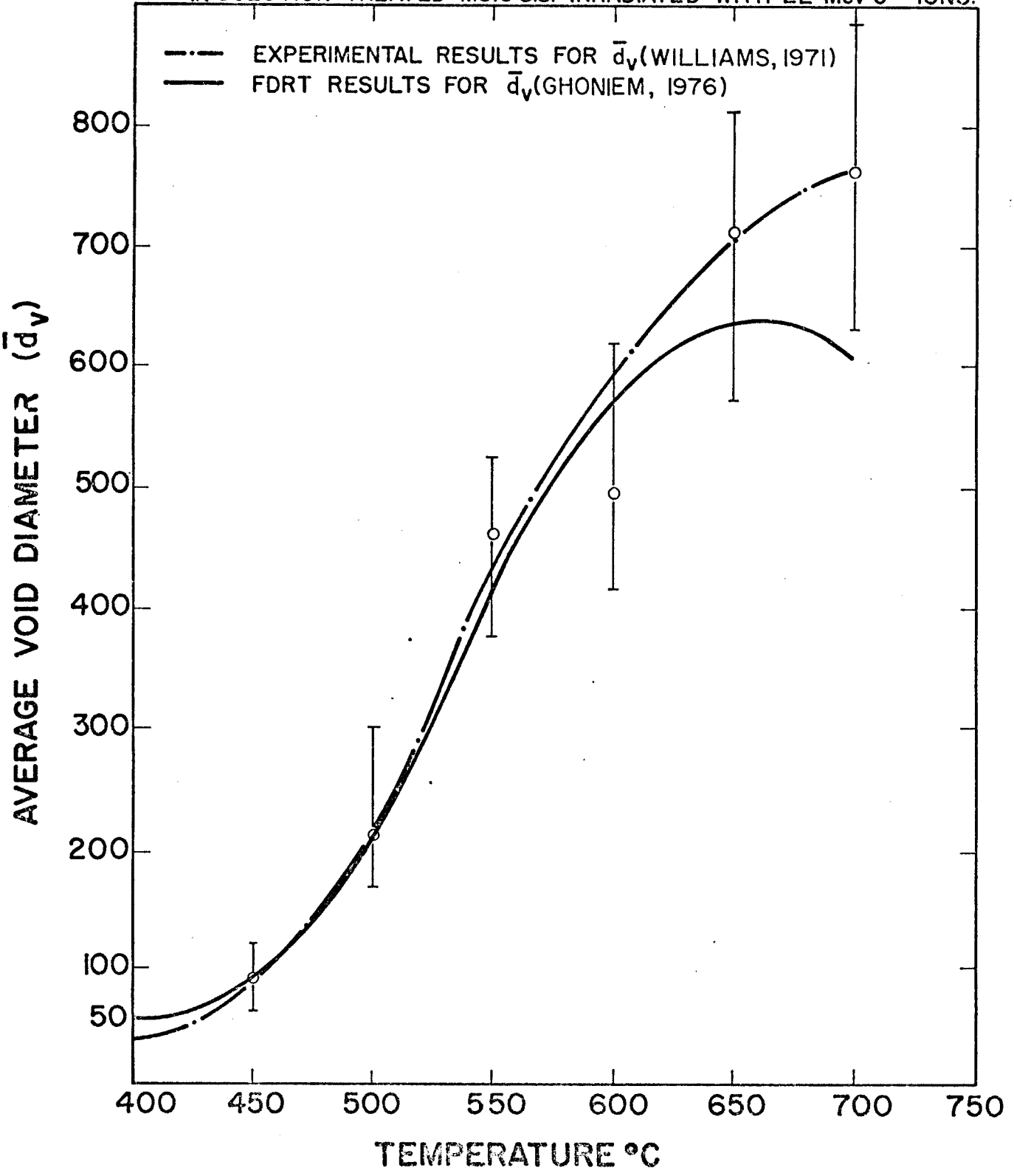

discussed later in detail. A comparison between computer simulations and experimentally measured void diameter as a function of temperature is shown in figure (12) and it reveals that the agreement between TRANSWELL and the data is quite good.

Two different views of a computer generated 3-dimensional plot of swelling as a function of dose and temperature are shown in figures (13-a) and (13-b). Note that the dose in all the curves shown is measured after the incubation dose. Figures (13-c) and (13-d) show the dose and temperature dependence of the mean void radius. It is interesting to note that at high temperatures voids grow very slowly at the beginning of irradiation due to a large vacancy surface emission rate and then they develop very fast once their size is large enough to reduce the vacancy emission rate to a negligible level.

Total vacancy emission rates in at./at./sec. are shown in figures (13-e) and (13-f). Three main features emerge from these figures: (1) vacancy emission rate is controlled mainly by dislocations at all temperatures and doses. (2) Emission rates of vacancies are very sensitive to temperature and they rise sharply at higher temperature. (3) As a first approximation, vacancy emission rates could be neglected compared to vacancy production rates in ion irradiated steel irradiated at high displacement rates.

The interstitial and vacancy sink removal rates are shown to be almost equal in magnitude at any given temperature and dose as shown in figures (13-g) and (13-h). The transient nature of removal rates at the start of irradiation (but after the incubation dose has been exceeded) could be easily seen from figures (13-g), (13-h) and (13-i). Some interesting features of the study of removal rates are summarized as follows:

(1) Quasi-steady state equilibrium conditions are satisfied rather quickly when the irradiation is started up after the incubation dose is exceeded.

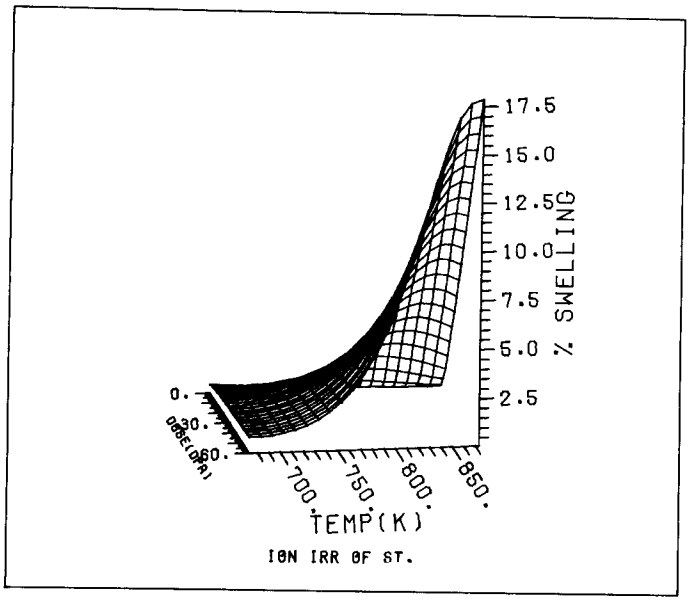

Fig. (13-a) Swelling in ion irradiated ST steel as a function of dose and temperature.

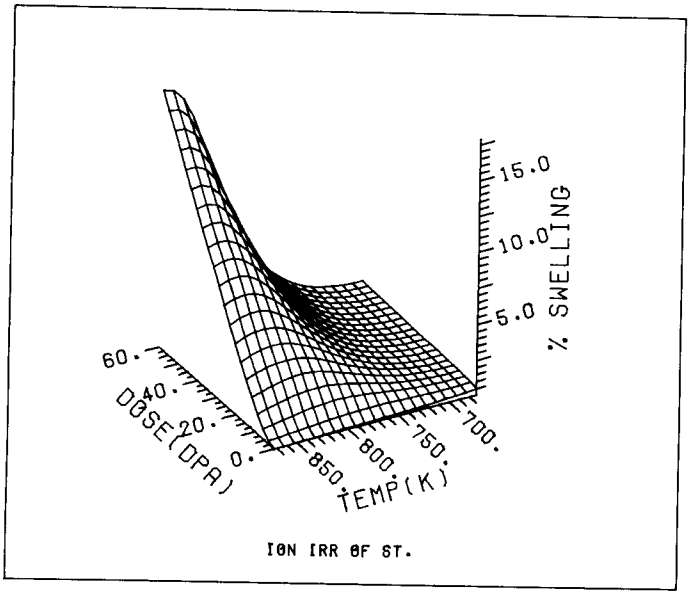

Fig. (13-b) Swelling in ion irradiated ST steel as a function of dose and temperature. (Different view of 13a).

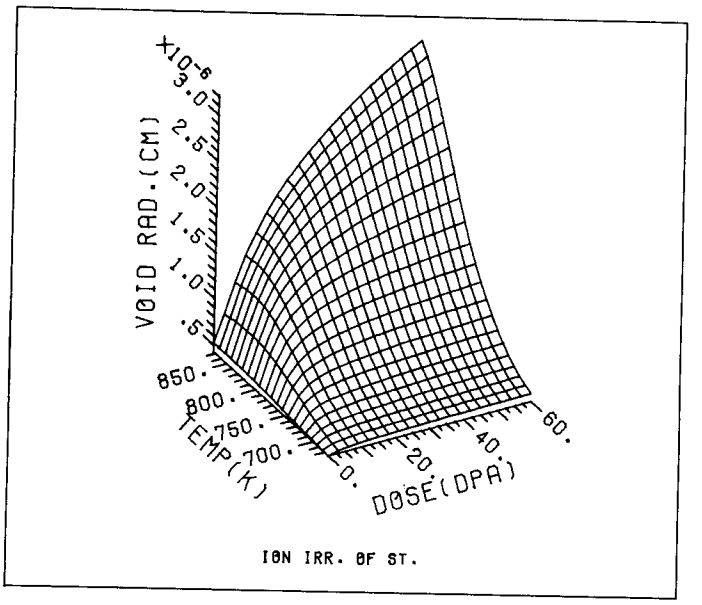

Fig. (13-c) Dose and temperature dependence of the mean void radius of ion irradiated ST S.S.

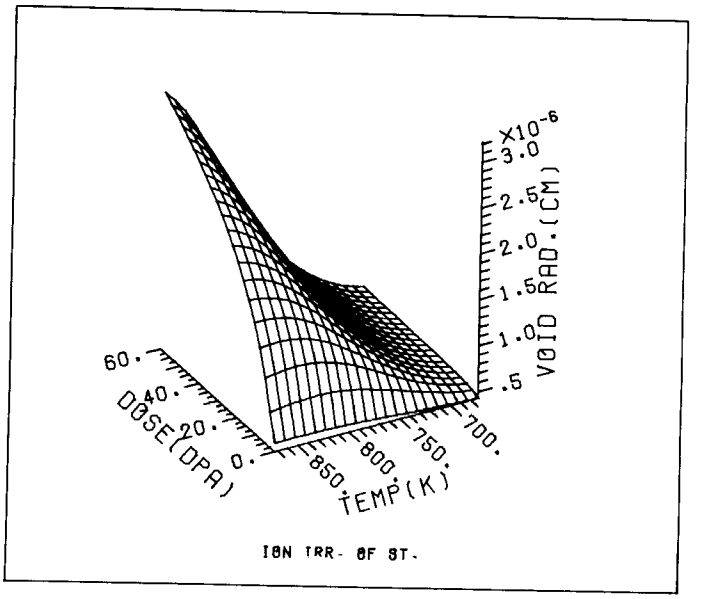

Fig. (13-d) Dose and temperature dependence of the mean void radius of ion irradiated ST S.S. (Different view of 13-c).

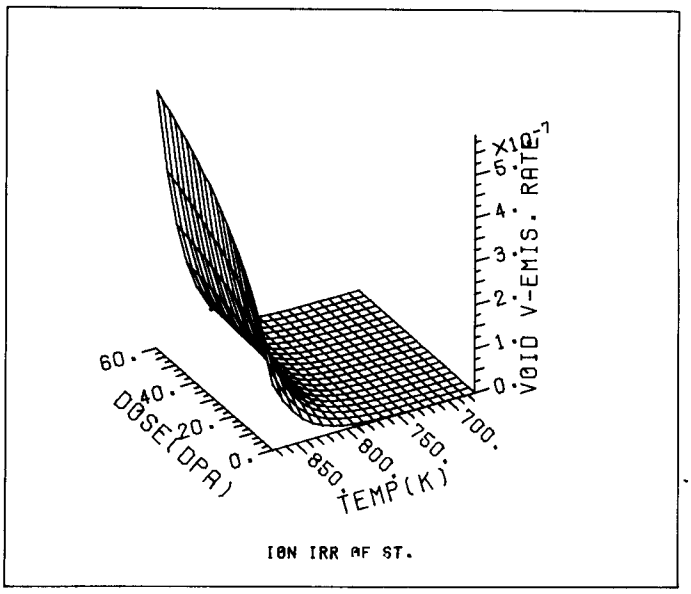

Fig. (13-e) Emission rate of vacancies from voids (at./at./sec.) as a function of dose and temperature.

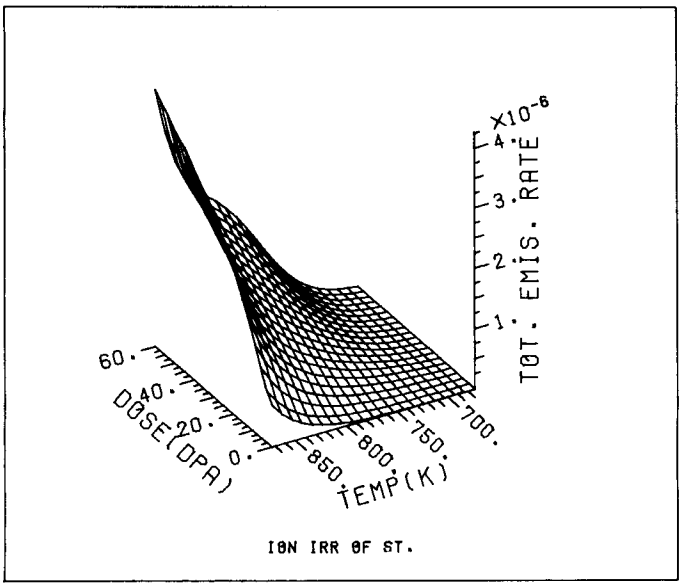

Fig. (13-f) Total vacancy emission rate from voids and and dislocations (at./at./sec) as a function of dose and temperature.

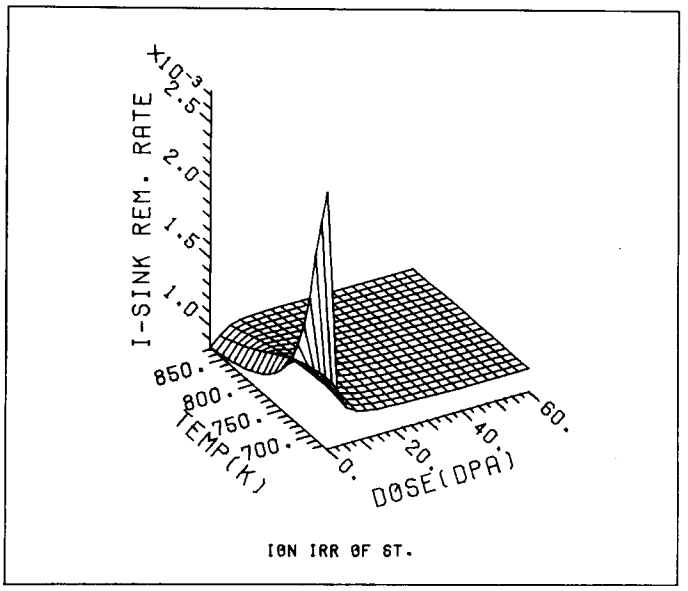

Fig. (13-g) Interstitial sink removal rate (at./at./sec) as a function of dose and temperature.

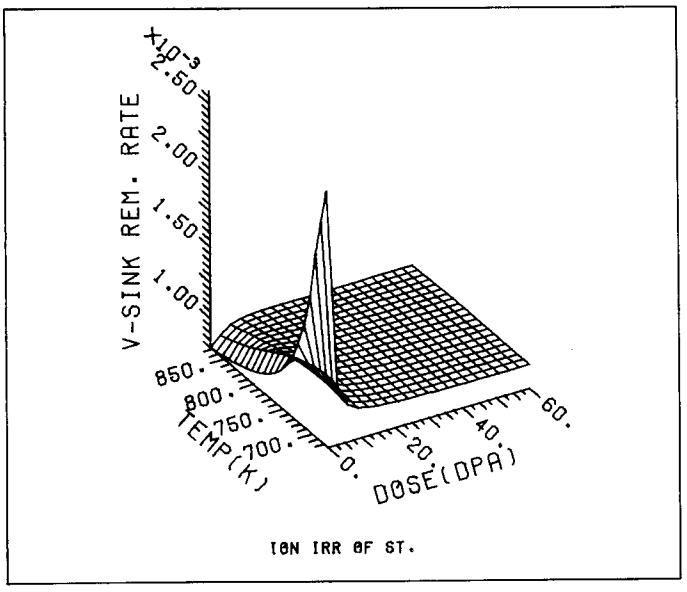

Fig. (13-h) Vacancy sink removal rate (at./at./sec) as a function of dose and temperature.

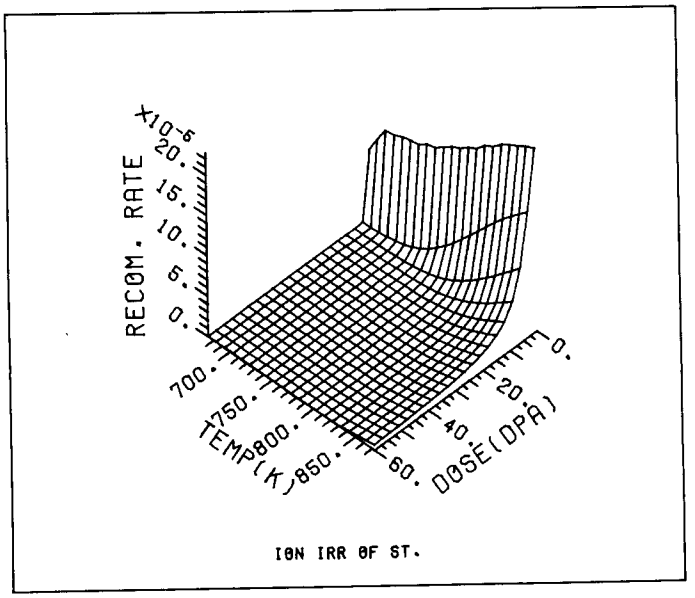

Fig. (13-i) Point defect recombination rate as a function of dose and temperature.

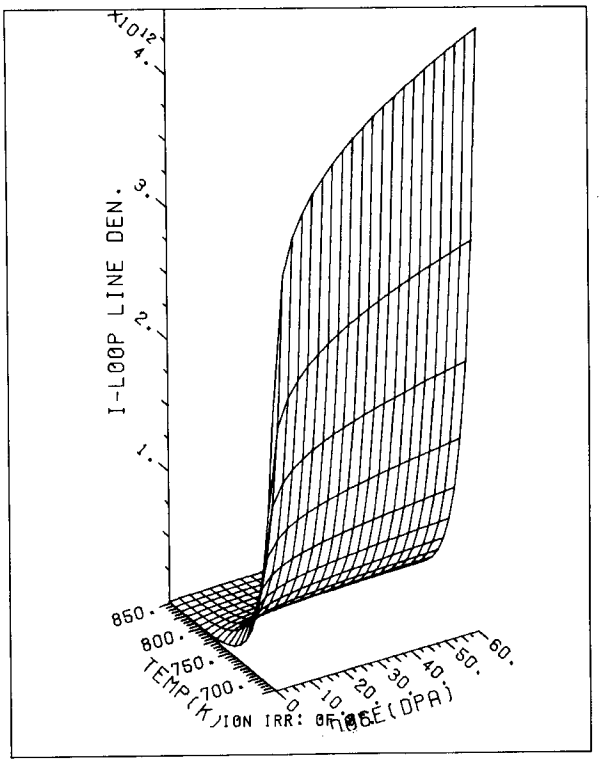

Fig. (13-j) Interstitial loop dislocation line density as a function of temperature and dose.

(2) At high temperatures and at the start of irradiation, sink removal rates are low and their magnitude increases with irradiation due to the build up of sinks (growth of both dislocation loops and voids).

(3) In ion irradiated steel, loss of point defects by recombination is totally dwarfed by their leakage to voids and dislocation loops. This result is clear when one compares the production rate (10^{-3} dpa/sec) with the loss rates of figures (13-g), (13-h) and (13-i).

Finally the interstitial loop line density in cm^2/sec as a function of dose and temperature is shown in figure (13-j). It is clear that reducing the irradiation temperature and increasing irradiation dose both have the effect of increasing interstitial loop line dislocation density. Note the more important effect of temperature due to sensitivity of nucleation to temperature.

ii) Electron Irradiation

Experimentally measured void concentrations as a function of temperature were, in this study, fitted to the expression:[10]

$$N_v^s = 6.5 \times 10^8 \exp \{1.0 \text{ eV}/kT\}$$

while interstitial loop number densities were calculated from the expression:

$$N_{i\ell}^s = 6.7 \times 10^{-3} \exp \{2.8 \text{ (eV)}/kT\}$$

Initial conditions were assumed as:

initial void radius = 40 Å

number of gas atoms in a void = 0 (no doping)

cascade efficiency = 0

while initial interstitial loop radius was calculated as in the previous section.

The temperature dependence of the swelling of ST 316 stainless steel under electron irradiation is compared with experiment in figure (14), while the

temperature dependence of the mean void diameter is compared with experiment in figure (15). The agreement in these figures is quite good but it must be emphasized that it is very sensitive to the value of t_i used. Changing the bias factor from 1.08 to 1.02 would drop the swelling at 500°C and 30 dpa by a factor of ~4. (See appendix A).

Three-dimensional plots for the temperature and dose dependence of swelling and mean void radius are shown in figures (16-a), (16-b), (16-c) and (16-d). It is noted that during electron irradiation, vacancies are more abundant than corresponding ion or neutron irradiations due to the lack of displacement cascades. As a consequence, the free-growth void radius at high temperatures can be smaller in electron than in ion or neutron irradiations.

Figures (16-e) and (16-f) show the different removal rates as a function of temperature and dose. An interesting feature of these graphs is that the recombination rate is important at high temperatures and unimportant at low temperatures. The total sink removal rate is shown to display the opposite effect. A possible explanation for this feature is the high initial sink density at low temperatures and the drastic effect of temperature on lowering the initial sink density at high temperatures. It is also seen that the total sink removal rate starts at a very low value at high temperatures and then increases with increasing dose due to the buildup of sinks (growth of loops and voids).

Average point defect concentrations are also affected by both temperature and dose. As an example, vacancy concentration in at./at. is shown in figure (16-g) as a function of dose and temperature. It is seen that increasing temperature has the effect of reducing vacancy concentration due to the higher mobility at higher temperatures. The high vacancy concentration at low temperatures and at the start of irradiation is assumed to be due to non-equilibrium circumstances at the start of irradiation.

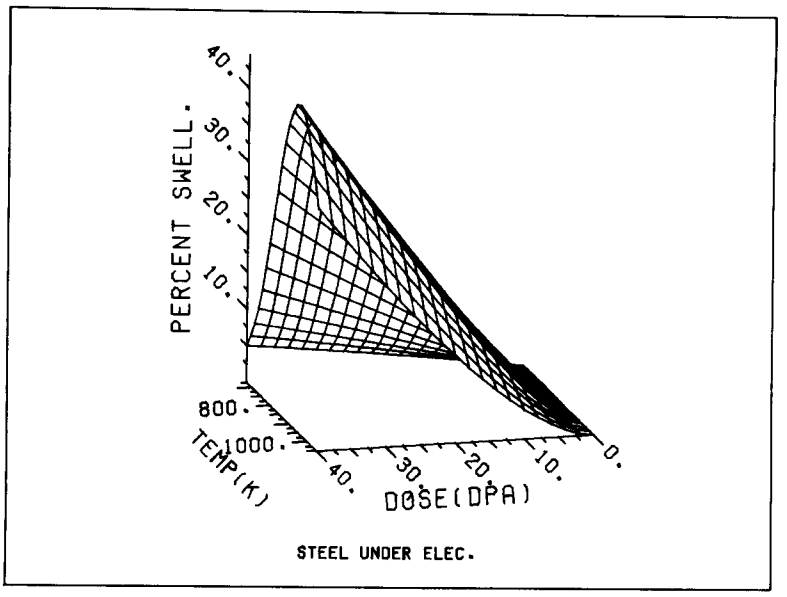

Fig. (16-a) Swelling of ST S.S. under electron irradiation as a function of dose and temperature.

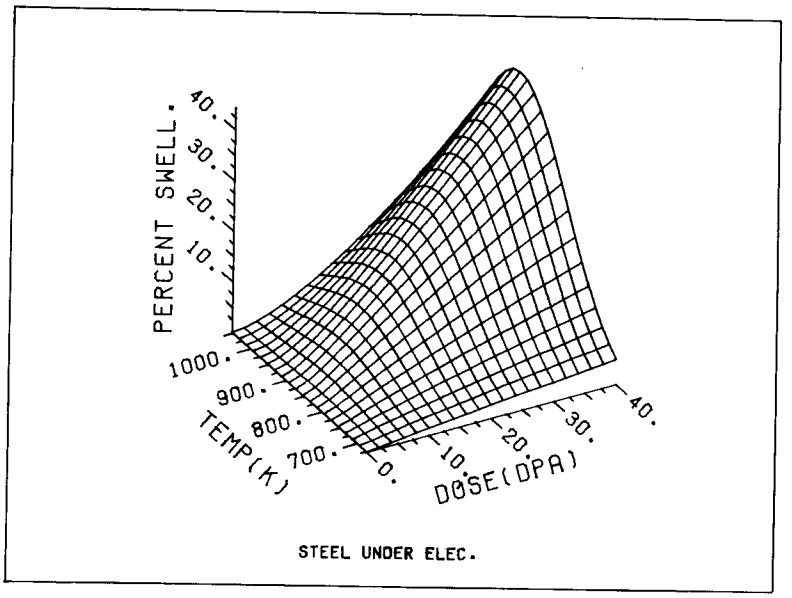

Fig. (16-b) Swelling of ST S.S. under electron irradiation as a function of dose and temperature.

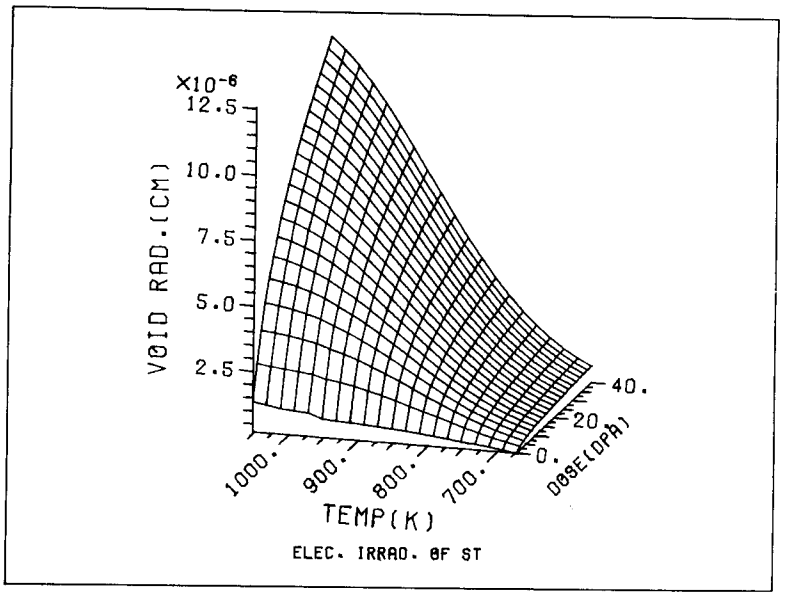

Fig. (16-c) Mean void radius as a function of dose and temperature in electron irradiated ST S.S.

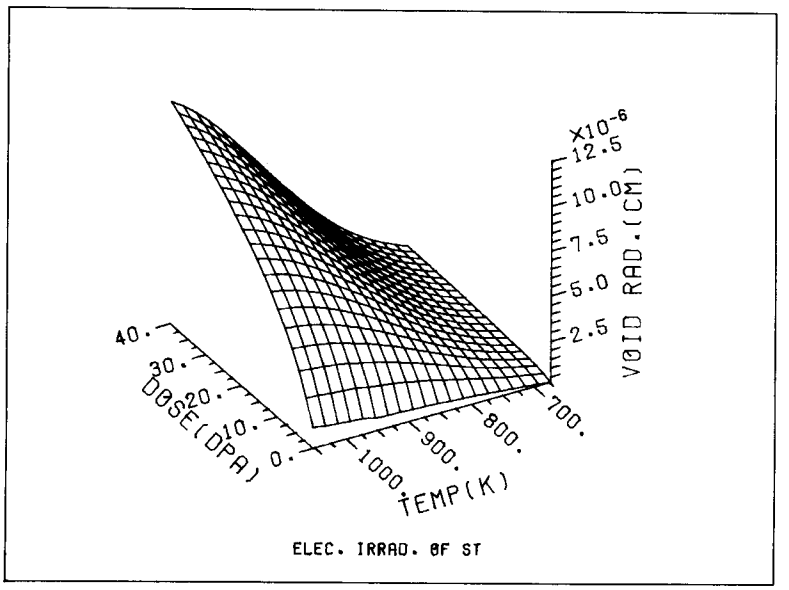

Fig. (16-d) Mean void radius as a function of dose and temperature in electron irradiated ST S.S.

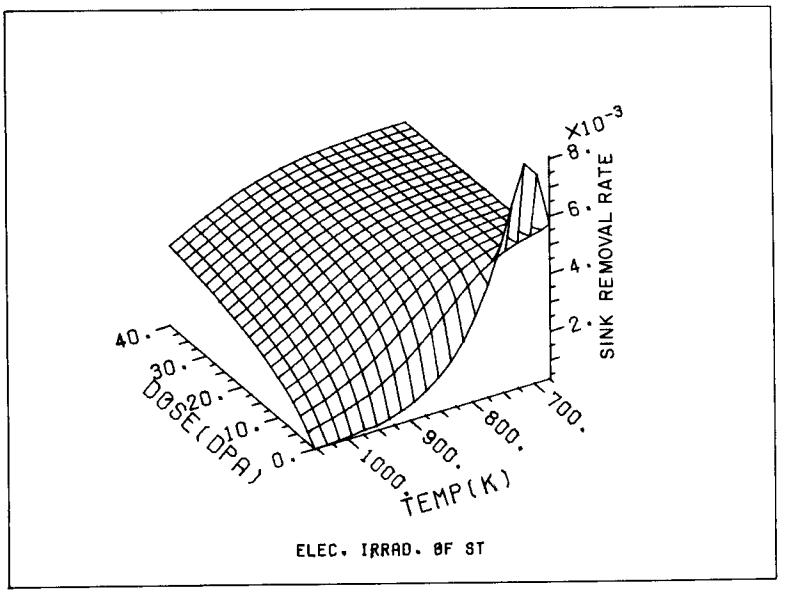

Fig. (16-e) Vacancy (or interstitial) sink removal rates (at./at./sec.) as a function of dose and temperature for electron irradiated ST S.S.

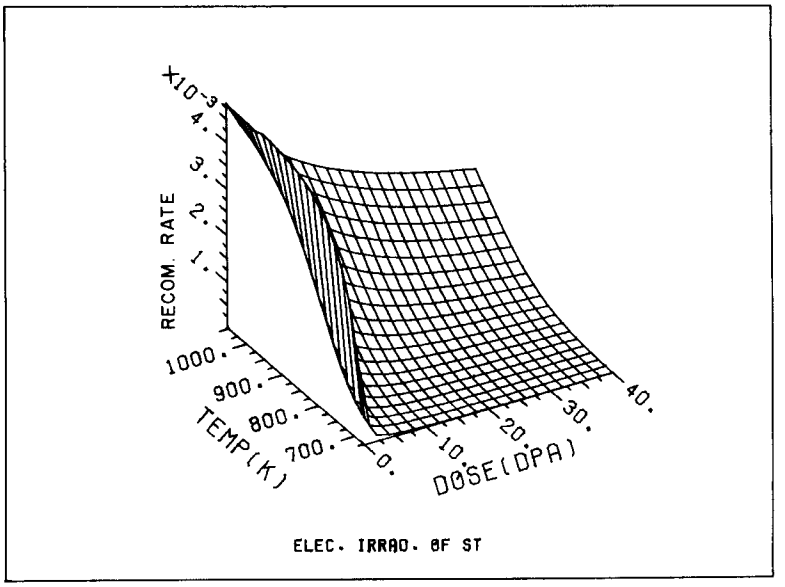

Fig. (16-f) Point defect removal rate (at./at./sec.) as a function of dose and temperature for electron irradiated ST S.S.

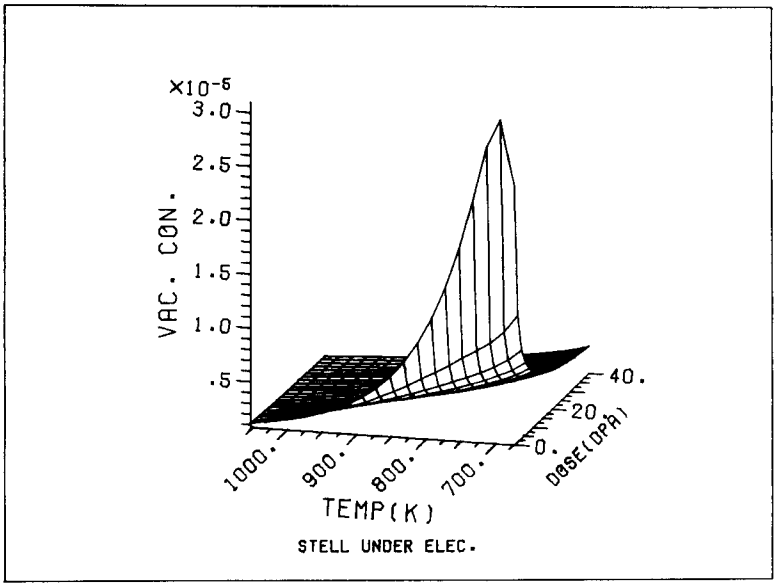

Fig. (16-g) Vacancy concentration (at./at./sec.) as a function of dose and temperature for electron irradiated ST S.S.

2.) Aluminum Irradiations

i) Neutron Irradiation

Packan's work[9] on neutron irradiated pure aluminum was analyzed using the parameters in table (5). Calculations of displacements per atom were made using HFIR fluxes (20) and Doran's (21) displacement cross sections with a threshold displacement energy of 16 ev for Al.[22] A value of 1.3 dpa was found to correspond to a fluence of 10^{21} n/cm^2/sec of neutrons with energy greater than 0.1 MeV.

The displacement rate was found to vary between 9.88×10^{-7} and 1.547×10^{-6} dpa/sec. Therefore, an average value of 1.3×10^{-6} dpa/sec was used in the calculations. Experiments on neutron irradiated aluminum (23, 24) indicated that the saturation void number density could be fitted to a simple expression as:

$$N_v^s = 2.8 \times 10^6 \exp \{0.55\ (eV)/kT\}\ \text{voids/cm}^3$$

which yields a value of $\sim 8 \times 10^{14}$ voids/cm^3 for aluminum at 55°C.

The following parameters were used in our TRANSWELL calculations:

number density of interstitial loops at saturation = 10^{14} cm^{-3}

initial deformation produced dislocation density = 10^9 lines/cm^2

initial number of gas atoms in a void = 50

gas production rate = 3×10^{-12} at./at./sec.

cascade efficiency (ε) = 10^{-3}

A dislocation loop-interstitial bias factor (Z_i) of 1.015 was found to fit very well both neutron irradiations and ion irradiations of aluminum and therefore, was used in these calculations.

Figure (17) shows the comparison between Packan's experiment and TRANSWELL calculations. Figure (18) shows the agreement between measured void sizes and

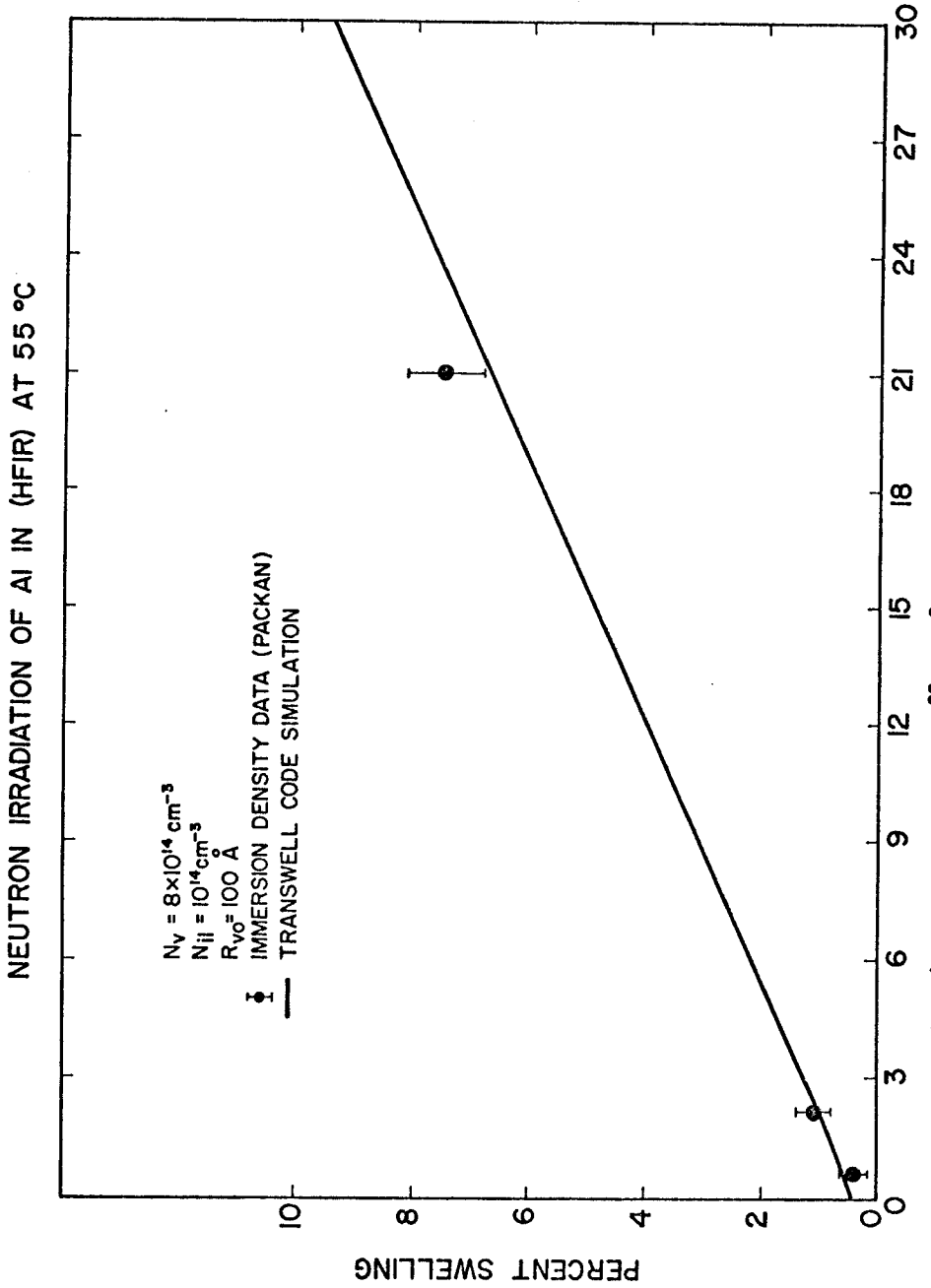

Fig. (17) Comparison between measured swelling of aluminum under neutron irradiation and theoretical predictions using TRANSWELL.

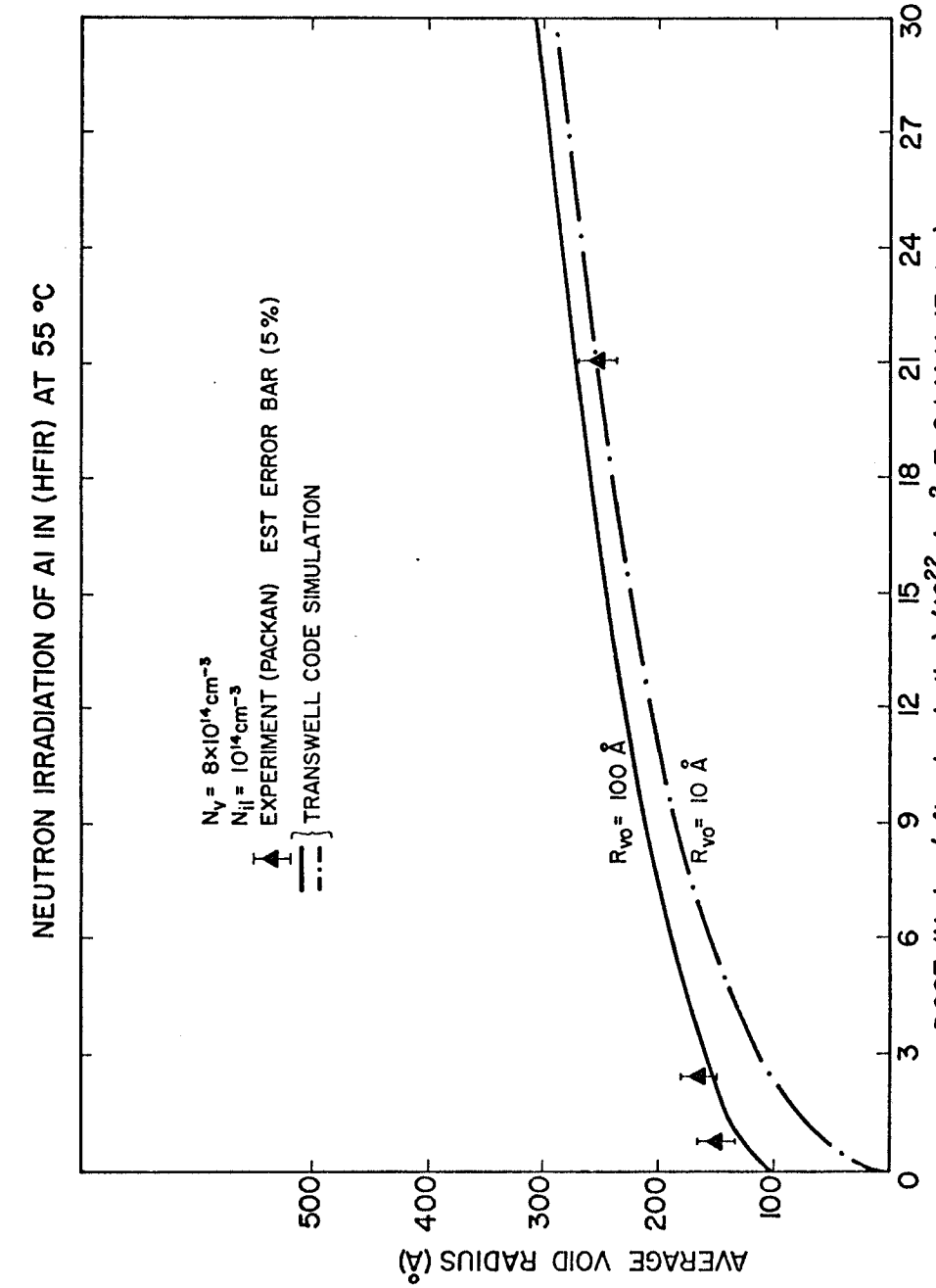

Fig. (18) Comparison between measured mean void radius of aluminum under neutron irradiation and theoretical predictions using TRANSWELL

computer calculated values if one starts with an observable void size (e.g., a radius of 100 Å). The agreement is shown to be still good even if the starting void radius is very small (e.g. 10 Å) indicating that the somewhat arbitrary choice of a free growth radius is not too restrictive in TRANSWELL.

ii) Ion Irradiation

The same set of material parameters used in neutron irradiated aluminum calculations were used in ion irradiations of aluminum with experimental conditions corresponding to Mazey's experiment (10).

The following set of initial conditions were used in the calculations:

$N_v^s = 1.26 \times 10^8 \exp\{0.55\ (eV)/kT\}$ voids/cm^3

$N_{i\ell}^s = 7.6 \times 10^8 \exp\{0.25\ (eV)/kT\}$ loops/cm^3,

and,

defect production rate	$= 10^{-3}$ dpa/sec
total displacements	= 104 dpa
initial deformation produced dislocation density	$= 10^9$ lines/cm^2
cascade efficiency	$= 10^{-3}$
initial number of gas atoms in a void	= 0
gas production rate	= 0 at./at./sec.
initial void radius	= 40 Å
Z_i	= 1.015

A comparison of TRANSWELL results to the experimentally determined swelling is shown in figure (19). The results of the work on aluminum seem to indicate the following, if reasonable agreement is to be attained:

a. A bias factor (Z_i) in the order of 1.015.

b. Aluminum is not as efficient as steel retaining vacancies in collision cascades.

c. Interstitial dislocation loop density changes slowly with temperature.

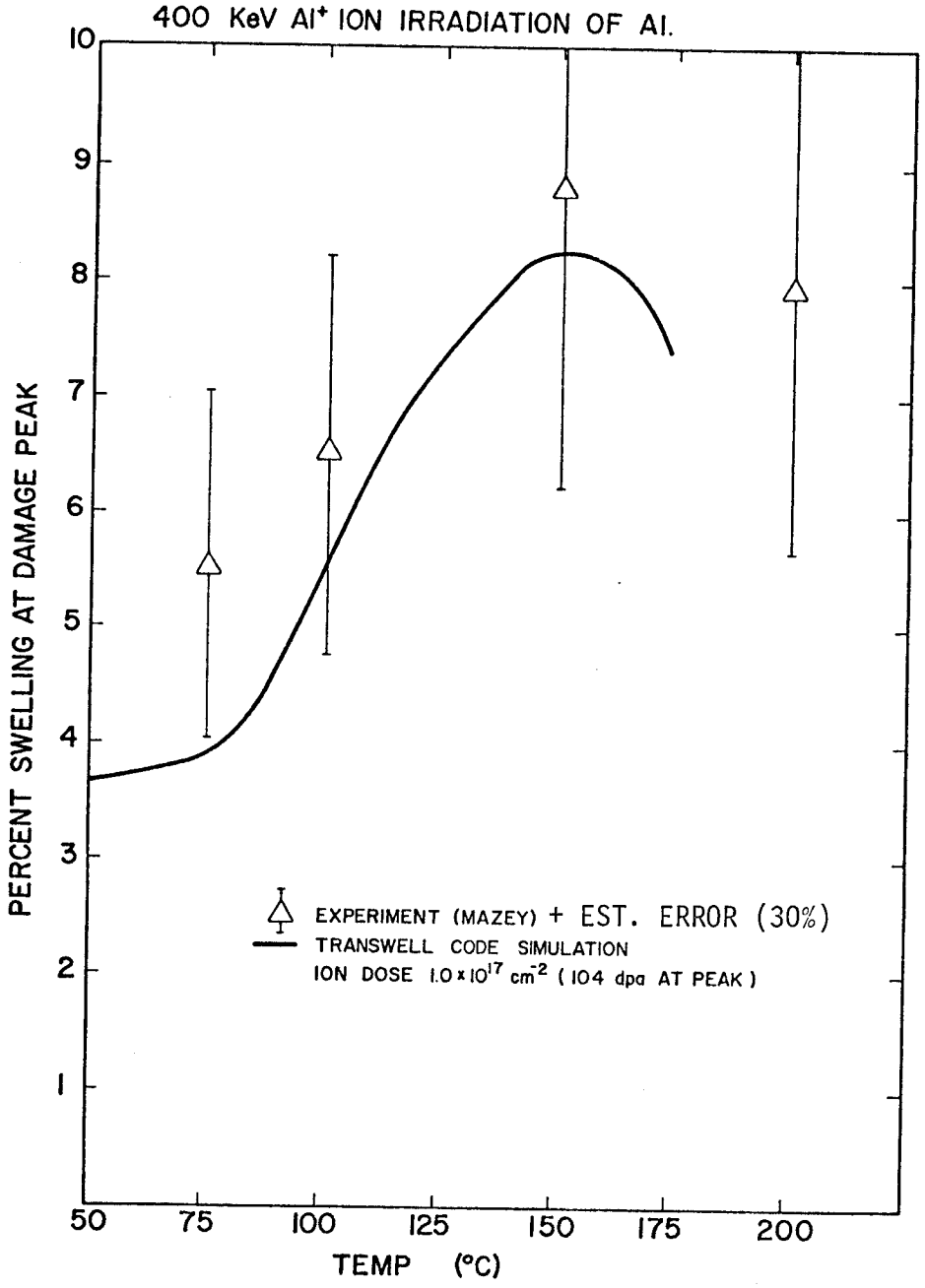

Fig. (19) Comparison between measured swelling in ion irradiated aluminum and theoretical predictions using TRANSWELL

Figures (20-a) and (20-b) show the percent swelling in aluminum under ion irradiation, while fig (20-c) shows the mean void radius, as a function of dose and temperature.

The line densities in lines/cm^2 are shown in figures (20-d), (20-e) and (20-f). The void equivalent sink density (defined as $4\pi r_v N_v$) is also demonstrated in figure (20-g).

In figures (20-h) and (20-i) thermal emission rates of vacancies from the surfaces of dislocations and voids are plotted as a function of dose and temperature. One can immediately see that the contribution of dislocations to the total emission rate is negligible at all temperatures and doses.

The recombination rate in figure (20-j) is again unimportant at low temperatures and becomes important at high temperatures. It also decreases with increasing irradiation time because of the growth of voids and loops. In figure (20-k) the interstitial sink removal rate displays the opposite behavior.

3.) Nickel Irradiations

i) Ion Irradiation

The following set of conditions were used in the computer simulation of swelling in nickel:

$$N_{i\ell}^s = 10^9 \exp\{1\ (eV)/kT\}\ cm^{-3}$$

total displacements = 13 dpa

production rate = 7×10^{-2} dpa/sec

initial void radius = 30 Å

cascade efficiency = 0.01

initial number of gas atoms = 0

gas production rate = 0

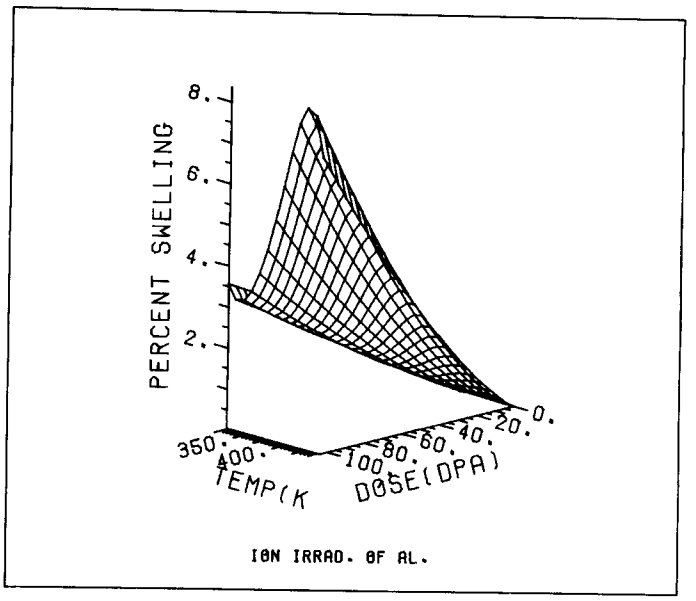

Fig. (20-a) Percent swelling in ion irradiated aluminum as a function of dose and temperature.

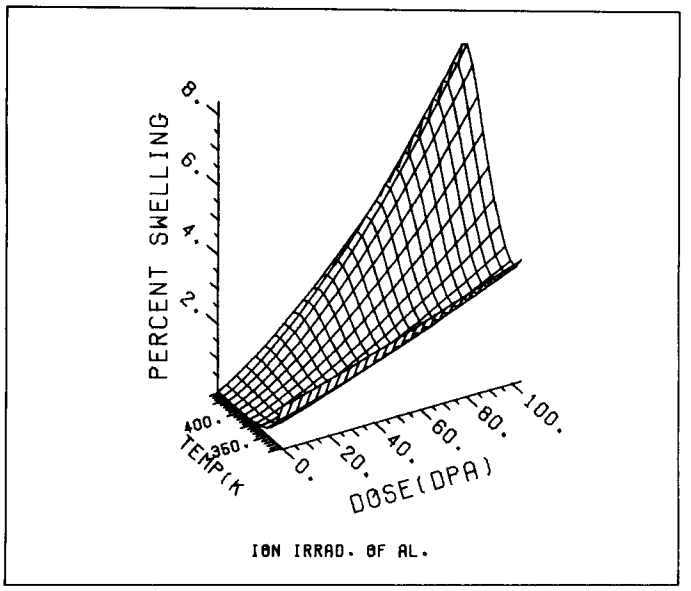

Fig. (21-a) Percent swelling in ion irradiated aluminum as a function of dose and temperature.

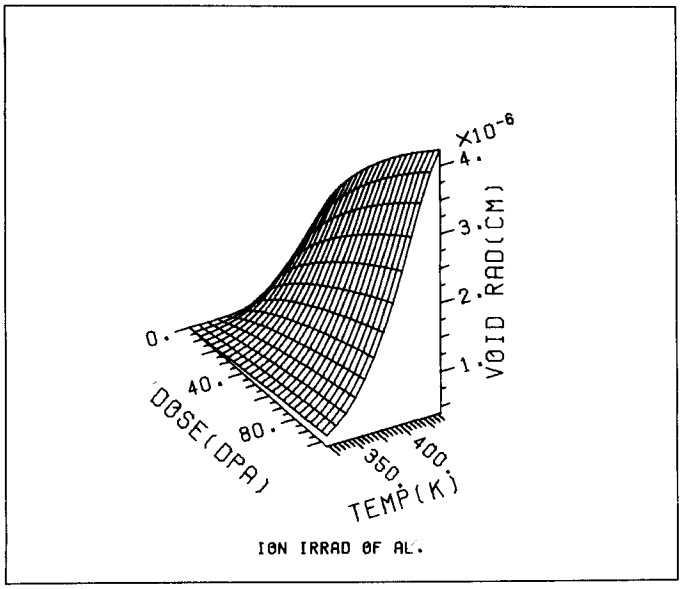

Fig. (20-c) Mean void radius in ion irradiated aluminum as a function of dose and temperature.

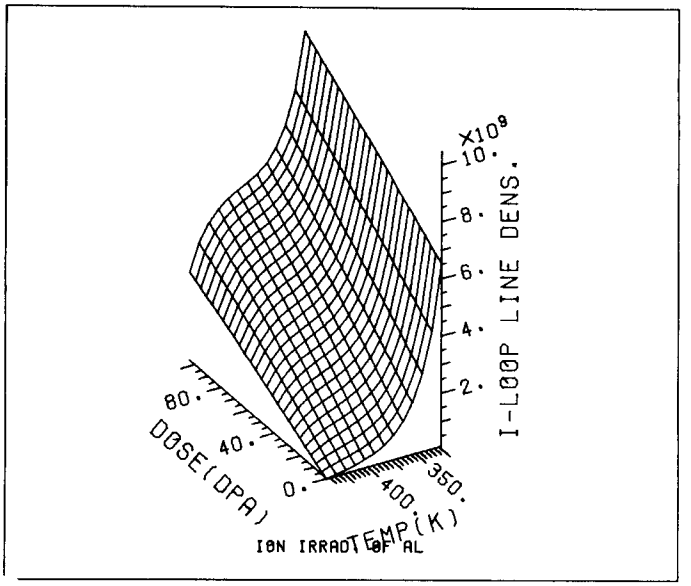

Fig. (20-d) Interstitial loop line density (cm^{-2}) in ion irradiated aluminum as a function of dose and temperature.

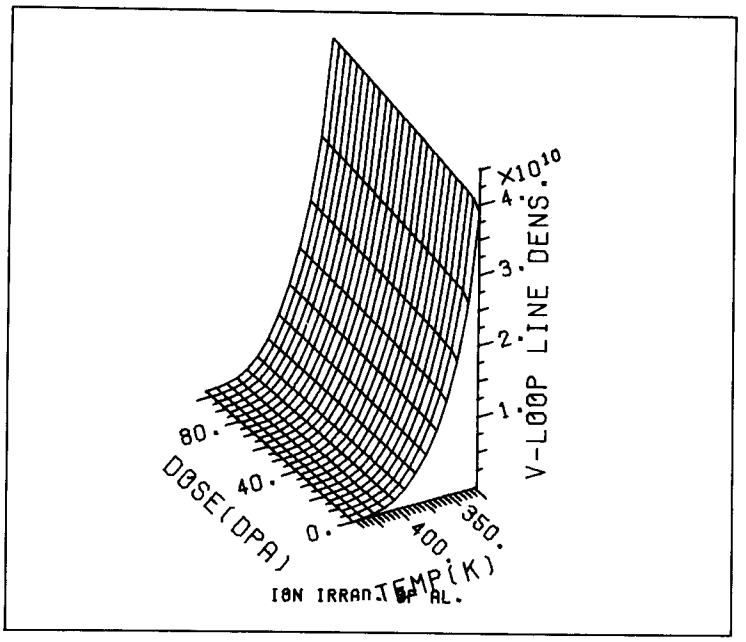

Fig. (20-e) Vacancy loop line denstiy (cm^{-2}) in ion irradiated aluminum as a function of dose and temperature.

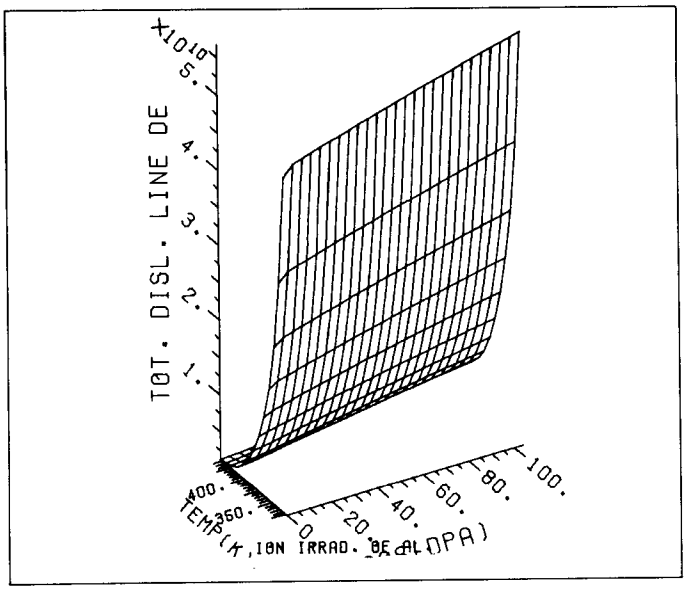

Fig. (20-f) Total line dislocation denstiy (cm^{-2}) in ion irradiated aluminum as a function of dose and temperature.

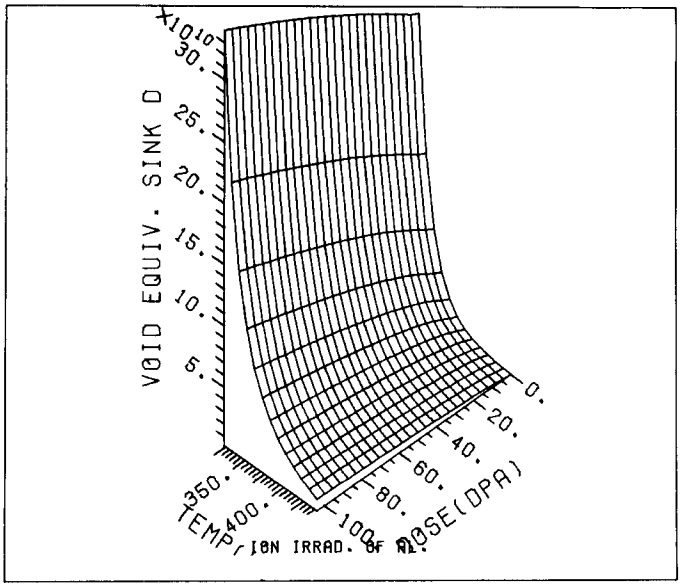

Fig. (20-g) Void equivalent sink density ($4\pi r_v N_v$ cm^{-2}) in ion irradiated aluminum as a function of dose and temperature.

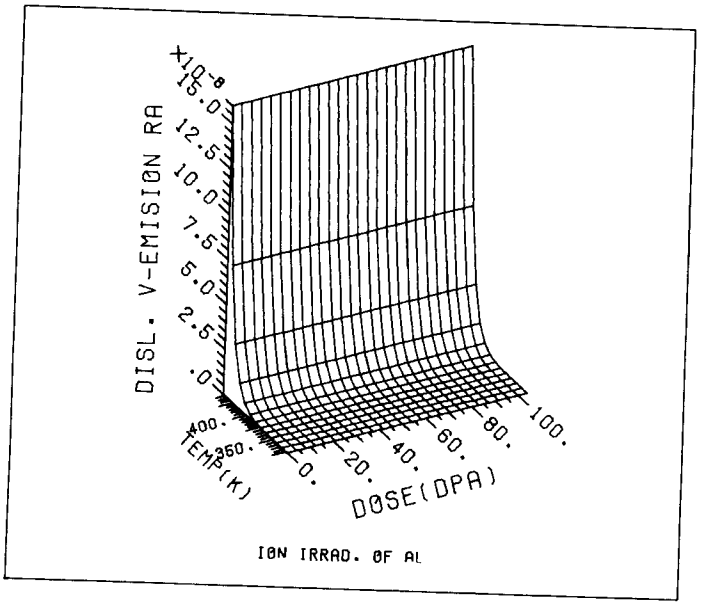

Fig. (20-h) Vacancy thermal emission rate from dislocations (at./at./sec) in ion irradiated aluminum as a function of dose and temperature.

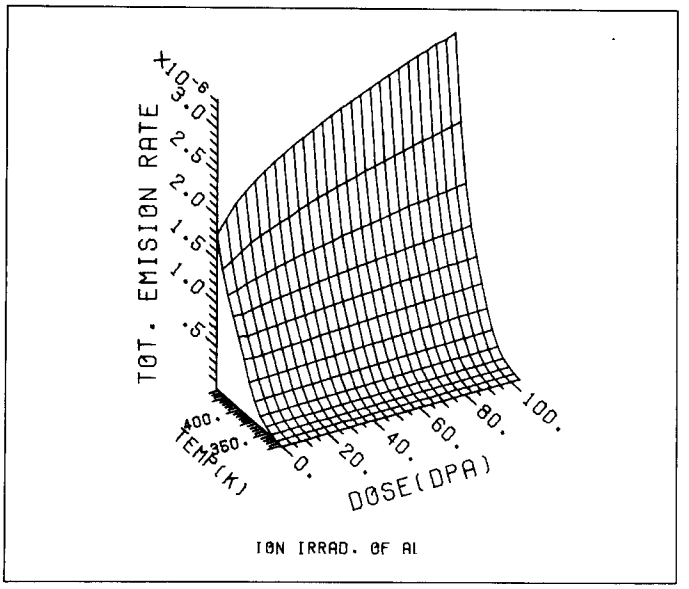

Fig. (20-i) Total vacancy thermal emission rate (at./at./sec) in ion irradiated aluminum as a function of dose and temperature.

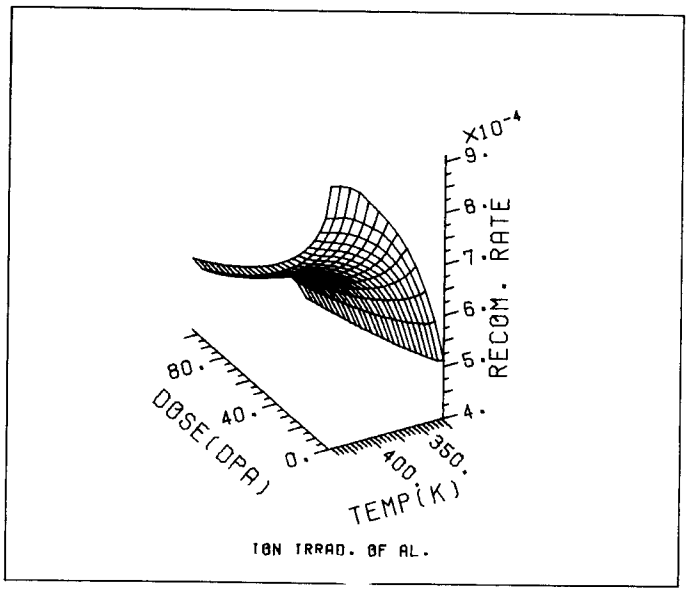

Fig. (20-j) Point defect recombination rate (at./at./sec) in ion irradiated aluminum as a function of dose and temperature.

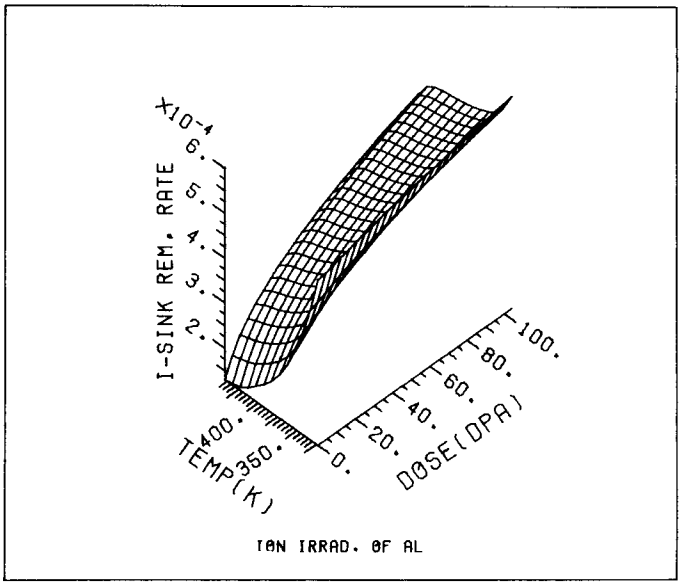

Fig. (20-k) Interstitial sink removal rate (at./at./sec) in ion irradiated aluminum as a function of dose and temperature.

initial deformation produced dislocation density = 10^8 lines/cm^2

interstitial-dislocation bias factor (Z_i) = 1.022

The experimentally measured void densities were used in all the computer calculations.

As shown in figure (21) there is good agreement between calculated swelling values and experimentally measured ones. Curve (2) shows the better agreement at high temperatures if the starting void radius was taken to be 200 Å. It was observed from all the calculations that small voids find it difficult to grow in ion or neutron irradiations without the assistance of gas for temperatures above the peak temperature. This suggested that the present growth theory could be better correlated with data at high temperatures if one starts with a "free-growth radius" as defined before. This radius, which is the radius of voids when nucleation has ceased, is obviously temperature as well as irradiation and microstructure dependent.

The important point to note from figure (21) is that TRANSWELL comes remarkably close to predicting the swelling in ion bombarded Ni from ~500°C to ~650°C under relatively high displacement rates (7×10^{-2} dpa/sec.)

ii) Electron Irradiations

Unfortunately, only total void induced swelling was reported in the electron irradiation studies of Ni, no void density, size or interstitial loop information was given.[12, 13] We have tried to simulate some of the irradiation parameters with those of steel at the same temperature even though we realize that there are some significant differences. At 450°C the following conditions were assumed for electron irradiated Ni.

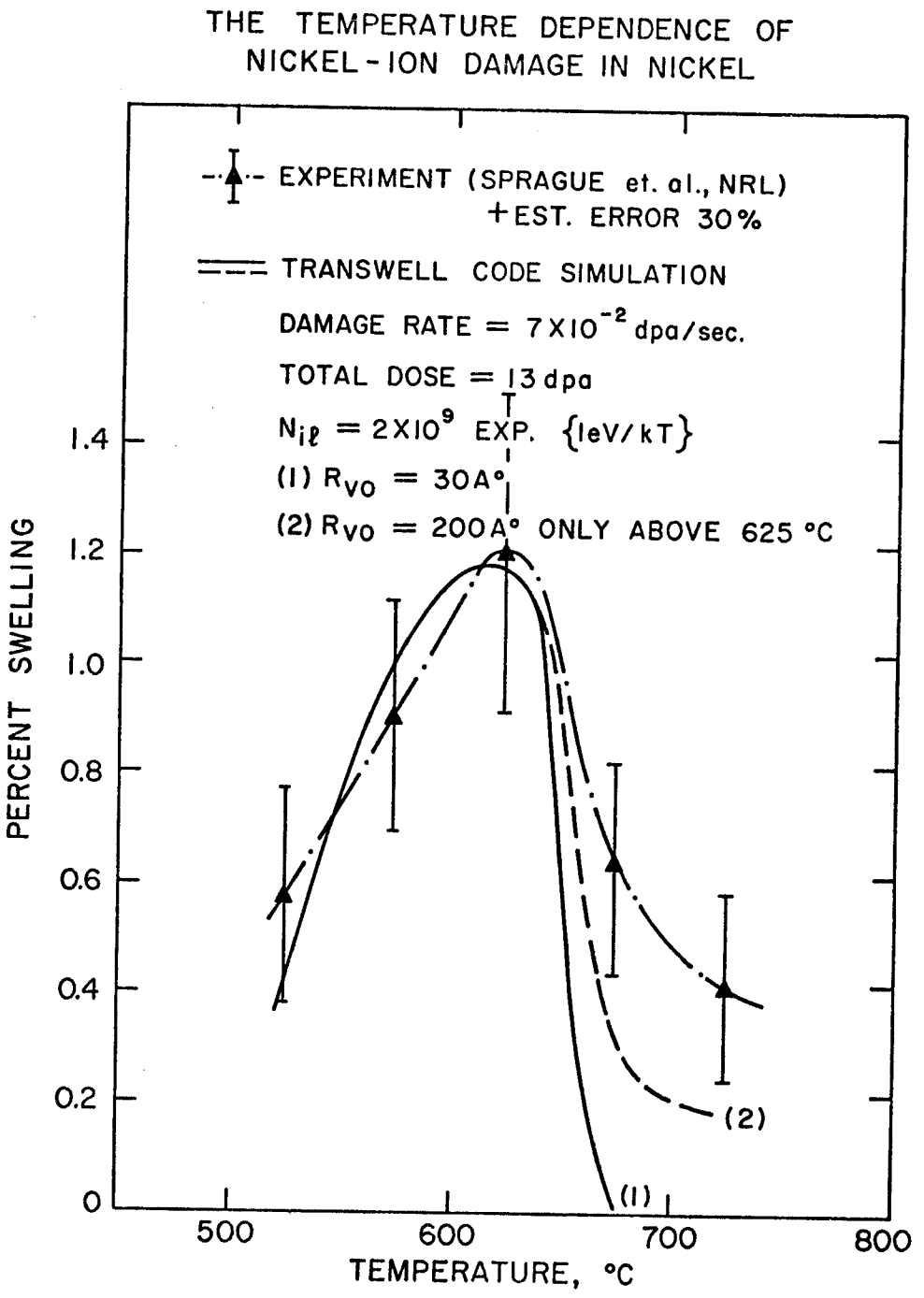
THE TEMPERATURE DEPENDENCE OF
NICKEL-ION DAMAGE IN NICKEL
EXPERIMENT (SPRAGUE et. al., NRL)
+EST. ERROR 30%
TRANSWELL CODE SIMULATION
DAMAGE RATE = 7X10^-2 dpa/sec.
TOTAL DOSE = 13 dpa
N_iℓ = 2X10^9 EXP. {1eV/kT}
(1) R_VO = 30A°
(2) R_VO = 200A° ONLY ABOVE 625 °C
PERCENT SWELLING
1.4
1.2
1.0
0.8
0.6
0.4
0.2
0
500
600
700
800
TEMPERATURE, °C
(1)
(2)

Fig. (21)

number of voids per cm^3 (saturation) = 8×10^{15}

number of interstitial loops per cm^3 (saturation) = 1×10^{15}

initial deformation produced dislocation density = 10^8 lines/cm^2

production rate = 2.06×10^{-3} dpa/sec.

total dose = 40 dpa

initial void radius = 10 Å

interstitial-dislocation loop bias factor (Z_i) = 1.022

With this set of parameters we found that computer simulations produce reasonable agreement with experimentally measured swelling values as shown in figure (22). At large doses foil surface effects impose artificial saturation limits on the swelling data so we would not expect TRANSWELL to agree in that region.

IV. C.) Annealing Experiments

One major constituent idea in pulsed irradiation studies is the allowance of voids to anneal out in between consecutive pulses. The accuracy of the model to predict this annealing behavior is crucial to the success of TRANSWELL in a pulsed simulation. The present investigation is aimed at focusing on this particular aspect and treating different factors that influence the annealing kinetics of voids.

The time rate of change of a void of radius R_v in a metal is given by (2):

$$\frac{dR_v}{dt} = \{D_v C_v - D_i C_i - D_v C_v^e \exp\{(\frac{2\gamma}{R_v} - P_g(R_v, Ng))\frac{\Omega}{kT}\}/R_v \qquad (1)$$

where,

D_v = vacancy diffusion coefficient, cm^2/sec.

D_i = interstitial diffusion coefficient, cm^2/sec.

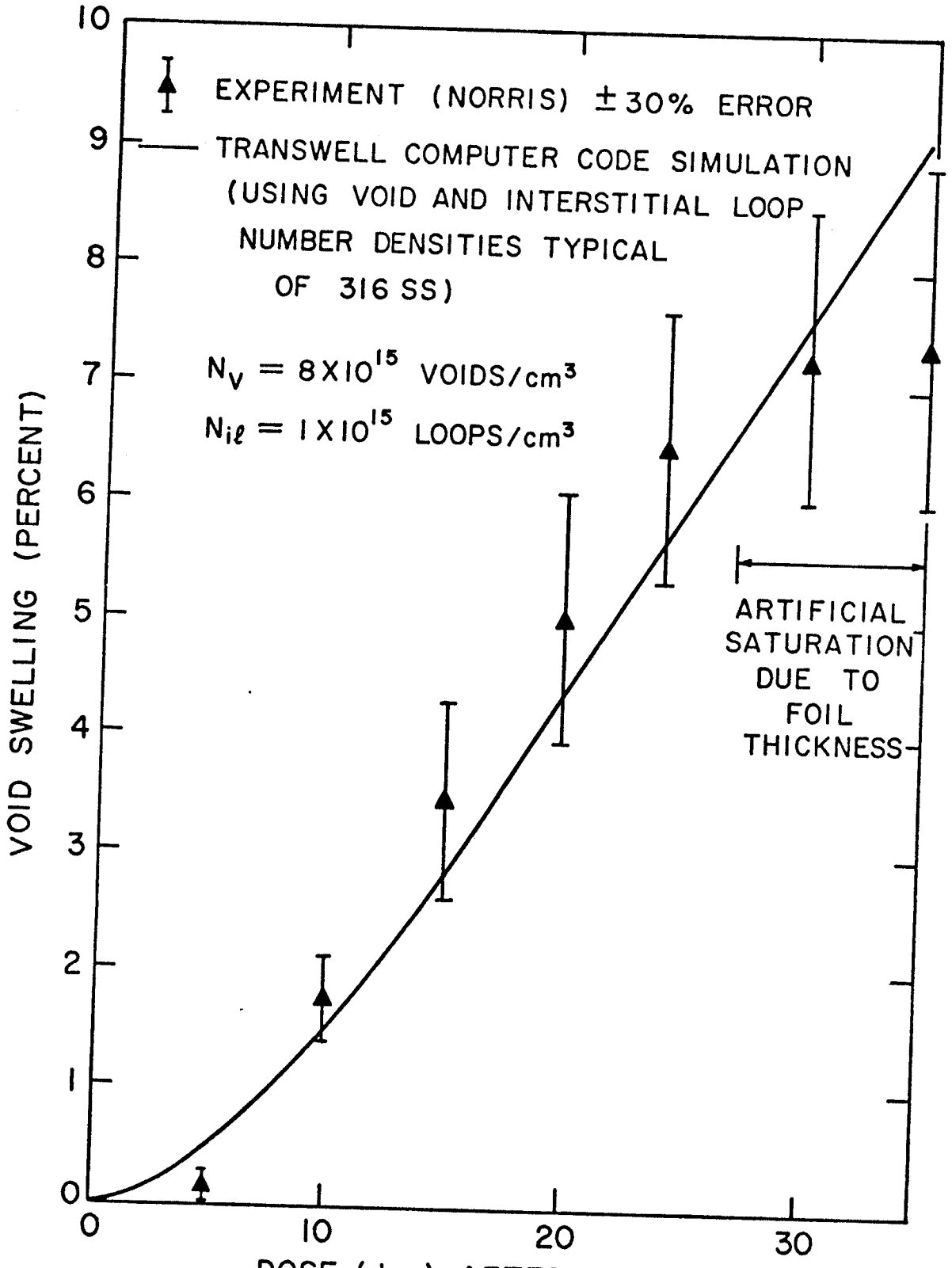

VOID SWELLING VERSUS DOSE AT 450°C IN NICKEL AT A DOSE RATE OF $2X10^{-3}$ dpa/sec (ELECTRON IRRADIATED)

Fig. (22)

C_v = vacancy concentration in the matrix (at./at.)

C_i = interstitial concentration in the matrix (at./at.)

$C_v^e = \exp(-E_v^f/kT)$

= thermal equilibrium vacancy concentration (at./at.)

γ = surface energy (eV/cm^2)

E_v^f = vacancy formation energy (eV)

k = Boltzmann's constant (eV/°K)

Ω = atomic volume (cm^3)

$$P_g(R_v,N_g) = \frac{3N_g kT}{4\pi(R_v^3 - 3b_v N_g/4\pi)} \qquad (2)$$

= gas pressure (ev/cm^3)

b_v = Van der Waal's constant cm^3/atom

N_g = number of gas atoms in the void

If there is no production of point defects, their concentrations will be the thermal equilibrium concentrations. In the annealing mode of voids, in between pulses, Equation (1) takes the simple form:

$$\frac{dR_v}{dt} = - D_v C_v^e \{\exp(\frac{2\Omega\gamma}{R_v kT}) - 1\}/R_v \ , \qquad (3)$$

provided that the void contains no gas atoms and the sink density is low in the metal.

From the last equation, it is clear that during annealing, voids emit vacancies to the surrounding matrix reducing their size.

In a number of experiments (14, 15) individual shrinkage curves were obtained for a number of voids at each temperature. This allowed isolation of a multitude of factors to affect void shrinkage, and was used to directly verify the last equation.

TABLE (6)

Parameters Used for Annealing Calculations

in Aluminum

E_v^m(eV)	= 0.57	(27)
E_v^f(eV)	= 0.65 - 0.665 *	
D_v^o(cm^2/sec)	= 0.045	(27)
γ(ergs/cm^2)	= 1000 *	
b (Å)	= 2.32	
Ω(cm^3)	= 1.25×10^{-23}	
C_v^e(at./at/) at 126°C	= 6.159×10^{-9} *	
C_v^e(at./at.) at 175°C	= 3.302×10^{-8} *	

*Used in present work

The presence of a void inside a crystal introduces an additional surface so that the surface energy γ provides a driving force to eliminate the voids. Annealing at temperatures high enough to permit self-diffusion causes the voids to shrink by emitting vacancies. The energy of a void, radius R_v, is reduced by an amount $(\frac{2\gamma\Omega}{R_v})$ per vacancy emitted. This leads to a concentration gradient of vacancies between the void and the vacancy sinks. In thin foils the foil surfaces are perfect sinks for vacancies and are thus able to maintain the vacancy concentration away from the voids at the thermal equilibrium level.

Fig. (23) shows the results of the TRANSWELL Computer Code simulations for voids in Al at 126°C (typical of Volin and Balluffi's experiments). A remarkably good agreement between experimental and computer simualtion values is obtained with a surface energy of γ = 1000 ergs/cm^2 and a vacancy formation energy E_v^f = 0.65 eV. Fig. (24) shows the predicted annealing behavior at a higher temperature (175°C) and a comparison with the experimental results of Westmacott, et. al.[14]. Values of γ = 1000 ergs/cm^2 and E_v^f = 0.665 eV are again found to produce good agreement. The slightly larger formation energy at the high temperature could be due to the presence of divacancies at this temperature. It is noted that the void anneals out about 30 times faster at the higher temperature than at the lower temperature.

A surface energy value of γ = 1000 ergs/cm^2 and a vacancy formation value of $E_v^f \tilde{=}$ 0.66 eV are established from the previous two experiments and substantiate the values that are used in the previous TRANSWELL equations for Al.

Neutron irradiated aluminum[25] showed a slower annealing behavior than quenched aluminum. There are numerous factors that could affect annealing kinetics such as transmutation products (both gaseous and solid)

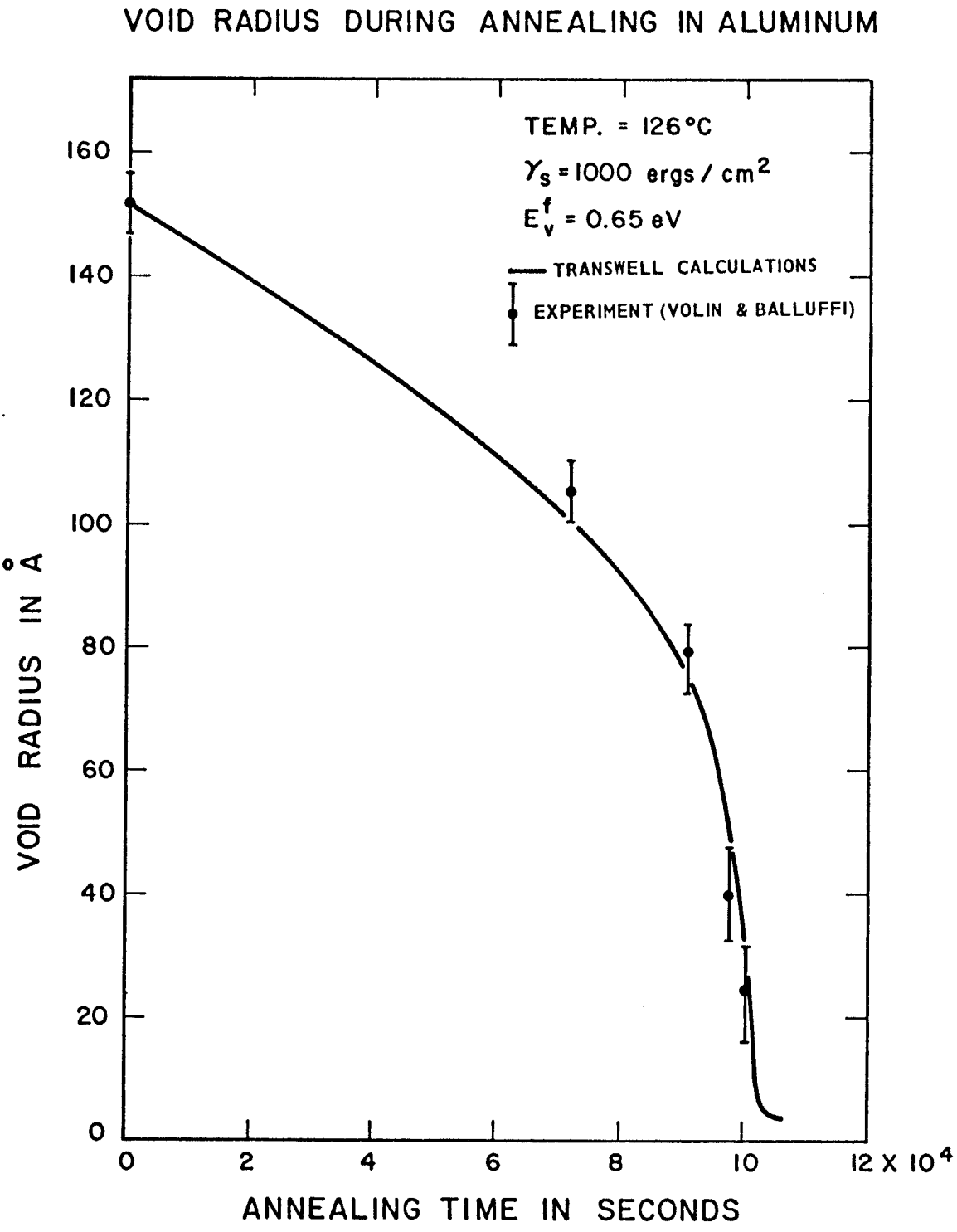
VOID RADIUS DURING ANNEALING IN ALUMINUM
TEMP. = 126°C
γ_s = 1000 ergs / cm^2
E_v^f = 0.65 eV
TRANSWELL CALCULATIONS
EXPERIMENT (VOLIN & BALLUFFI)
VOID RADIUS IN Å
0
20
40
60
80
100
120
140
160
0
2
4
6
8
10
12 X 10^4
ANNEALING TIME IN SECONDS

Fig. (24)

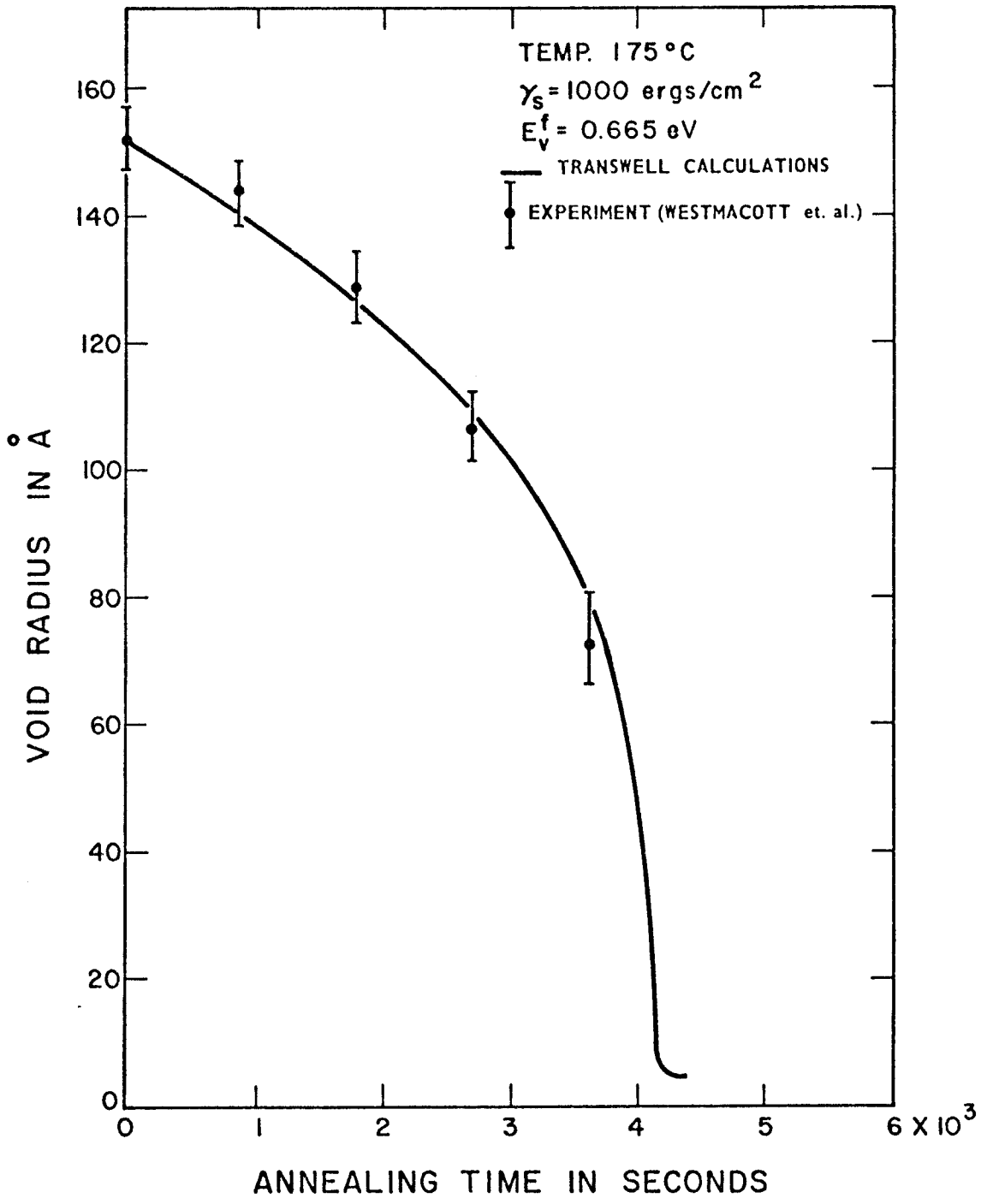
TEMP. 175°C
γ_s = 1000 ergs/cm^2
E_v^f = 0.665 eV
TRANSWELL CALCULATIONS
EXPERIMENT (WESTMACOTT et. al.)
VOID RADIUS IN Å
160
140
120
100
80
60
40
20
0
0
1
2
3
4
5
6 X 10^3
ANNEALING TIME IN SECONDS

Fig (25)

and absorption of vacancies by other voids. Due to the importance of inter-pulse annealing in Pulsed Systems, study of the sensitivity of annealing kinetics to those factors are investigated in reference (26).

V. Discussion

The results of the present comparisons between TRANSWELL and experimental data have shown that the FDRT can do a remarkably good job of predicting the high temperature void swelling behaviour of both pure elements and alloys. The fact that TRANSWELL can predict the temperature dependence of defect parameters over a wide range of displacement rates ($\sim 10^{-6}$ to $\sim 10^{-1}$ dpa/sec) and with different bombarding species (neutrons, heavy ions and electrons) is also very satisfying. However, the reader must remember that this FDRT only applies to the situation when an equilibrium void and interstitial loop density is established, i.e., it does not apply to the initial stages of irradiation when nucleation is still dominant.

There is some problem with TRANSWELL at very high temperatures ($> 0.4 - 0.45\ T/T_m$). This difficulty arises because the initial void size has to be relatively large to withstand the emission of vacancies which is proportional to 1/r. One way to fix this problem would be to use an empirically determined void size at saturation which is a function of temperature. It is clear that initial radii of 10 Å is satisfactory at low temperature (~ 0.3 T/Tm), but at temperatures above T/Tm $\tilde{=}$ 0.4 this should increase to several hundred angstroms. Future work will be aimed at determining a simple way to handle this problem.

The use of different spike collapse efficiencies (4.4% for steel, 0.1% for Al and 1% for Ni) to achieve agreement between theory and experiment reveals again that the displacement cascade in Al is rather diffuse and inefficient at retaining vacancies.

It is not known whether the difference between ε's for 316 SS and Ni are significant at this time but analysis of future experimental data will concentrate on this point.

It will also be noticed that slightly different values of the bias factor of dislocations for interstitials were used.

Material	Zi
316 SS	1.08
Al	1.015
Ni	1.022

The sensitivity of the final defect parameters to this term was not studied here and will be a part of a general sensitivity study in a future paper. However, one would expect that since the interaction depends on the strain energy, and since that depends on the shear modulus, different values of Z_i should be assigned different materials. We cannot comment further on this here but future studies will certainly need to take this into account.

Finally, we have included a large amount of auxillary data, without comment, from the TRANSWELL code. This information is displayed in three dimensional plots and obviously can be very valuable in explaining other phenomena in metals (creep, yield strength and maybe even blistering). The magnitude of this data was described in a previous document and the significance will be explored in a future publication.

VI. Conclusion

The results of this study show that TRANSWELL can accurately predict the post incubation growth behaviour of voids and dislocation loops as a function of temperature in a wide variety of materials irradiated over a factor of 10^5 in steady state displacement rates with two widely, different types of irradiation. The TRANSWELL code also accurately predicts the annealing of voids in dilute solutions indicating that it can adequately predict the behaviour between pulses of irradiation.

Acknowledgement

This research was supported by a grant from the Electric Power Research Institute, Palo Alto, California.

References

1. A. D. Brailsford and R. Bullough, J. Nucl. Mat. 44 (1972), 121.

2. N. Ghoniem and G. Kulcinski, Univ. of Wis. Fusion Design Memo, UWFDM-180 (1976).

3. N. Ghoneim and G. Kulcinski, Univ. of Wis. Fusion Design Memo, UWFDM-181 (1976).

4. R. Bullough, B. L. Eyre and R. Krishan, Proc. R. Soc. Lond. A.346, (1975) p. 81.

5. A. Taylor et al., Investigation of Pulsed Ion Irradiation on Void Microstructure, ANL Quarterly Report, Jan.-March 1975, ANL/CTR/TM-39.

6. J. A. Sprague and F. A. Smidt, Jr., NRL, NRL Memorandum Report 2629, August 1973, p. 27.

7. T. W. Williams, Proc. of B.N.E.S. Conf. on Voids Formed by Irradiation of Reactor Materials (ed. D. F. Pugh, M. H. Loretto and J. H. Harris) (1971).

8. M. J. Makin and G. P. Walters, Proc. of Conf. on Physics of Voids (ed. by R. S. Nelson), published as Harwell Report, AERE R-7934 (1975).

9. N. H. Packan, J. Nucl. Mat. 40 (1971), 1.

10. D. J. Mazey, R. Bullough and A. D. Brailsford, Harwell Report AERE-R 8344 (1976).

11. J. A. Sprague, J. E. Westmoreland, F. A. Smidt, Jr. and P. R. Malmberg, J. of Nucl. Mat. 54 (1974), 286.

12. D. I. R. Norris, Phil. Mag., Vol. 23, No. 181, p. 135, Jan. 171.

13. D. I. R. Norris, Phys. Stat. Sol. (a), 4, K5 (1971).

14. K. H. Westmacott, R. W. Smallman and P. S. Dobson, Metals Science Journal, March 1968, p. 177.

15. T. E. Volin and R. W. Baluffi, Phys. Stat. Sol. 25, 163 (1968).

16. S. D. Harkness and C. Y. Li, Rad. Damage in Reactor Materials, Vol. II (1969), p. 189, IAEA, Vienna.

17. H. Wiedersich, Rad. Effects, Vol. 12 (1972), p. 111.

18. R. W. Conn, S. Abdel-Khalik, G. A. Moses, E. T. Cheng, C. Cooper, J. Howard, G. L. Kulcinski, E. Larsen, E. Lovell, G. Magelssen, I. Sviatoslavsky, W. Wolfer, F. Beranek, S. K. Chang, R. Droll, N. Ghoniem, T. Hunter, M. Ortman, R. Spencer, G. Shuy, M. Ragheb, Univ. of Wis. Fusion Design Memo, UWFDM-190 (1976).

19. T. S. Lundy and J. F. Murdock, J. Appl. Phys. 33, 1671 (1962).

20. Doran, D. G. and Graves, N. J., Hanford Eng. and Development Lab. Report, HEDL-TME 76-70, VC-79 b, d , Dec. 1976.

21. Doran, D. G., Nucl. Sci. Eng. 52, 398, 1973. See also Nucl. Sci. Eng. 49, 130, 1972.

22. Kulcinski, G. L., Doran, D. G. and Abdou, M. A., UWFDM-15, Univ. of Wisconsin, Madison, Wisconsin, February, 1973.

23. Stiegler, J. O., Radiation Induced Voids in Metals, Proc. of the 1971 International Conf. at Albany (Edit. J. W. Corbett and L. C. Ianiello), p. 326 (1972).

24. Adda, Y., Radiation Induced Voids in Metals, Proc. of the 1971 International Conf. at Albany (Ed. J. W. Corbett and L. C. Ianello), p. 36 (1972).

25. Smallman, R. E. and Westmacott, K. H., British Nuclear Energy Society, European Conference Proceedings (1971), p. 159.

26. N. Ghoniem and G. L. Kulcinski, Univ. of Wisconsin Fusion Design Memo, UWFDM-199 (1977).

27. Seeger, A., J. Phys. F. Metal Physics, 3(2), 248 (1973).

APPENDIX A

COMBINED EFFECT OF CASCADE COLLAPSE EFFICIENCY AND BIAS FACTOR ON VOID SWELLING IN ION IRRADIATED 316 SS

Because of the importance of the collision cascade collapse in ion or neutron irradiated metals, this appendix will discuss the combined effect of changing the collapse efficiency (ε) and the bias factor (Z_i), on swelling of 316 SS.

The calibration of the experimental results of ion irradiated 316 SS in Chapter IV , considered values of Z_i = 1.08 and ε = 4.4%. This combination of Z_i and ε allowed the theory to correlate with the experimental results. Similar calculations have been carried out, with the following conditions:

$$\text{Dose rate} = 10^{-3}\text{dpa/s},$$

$$\varepsilon = 1.2\%,$$

$$Z_i = 1.025,$$

$$R_c(0) = 300\ \text{Å at } 700°C,$$

$$R_c(0) = 30\ \text{Å at } 450°C,$$

and the parameters of 316 SS from Table (6.1).

The temperature dependence of the swelling is shown in Figure (A.1). It can be seen that the theory comes close to the experimental values, even with a different combination of ε and Z_i. This indicates that the individual choice of Z_i and ε is not unique to produce agreement with experimental results, only the combination of both.

THE TEMPERATURE DEPENDENCE OF VOID SWELLING IN M316 S.S. IRRADIATED WITH 22 MeV C^{++} IONS.

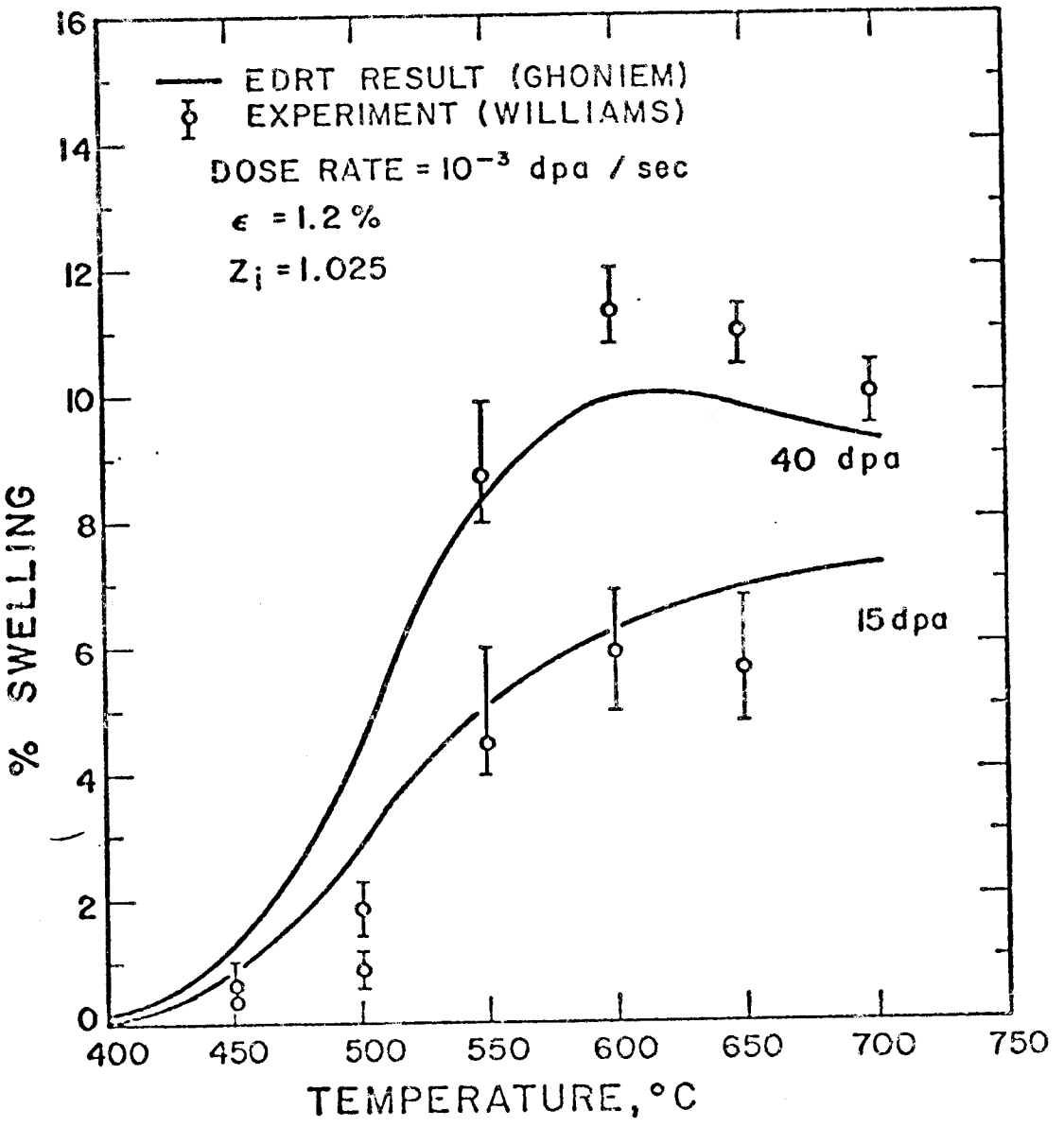

Fig. (A.1)